8736 *Inorg. Chem.* **2009**, *48*, 8736–8750
DOI: 10.1021/ic900908n

Inorganic Chemistry
Article

Variable Coordination Behavior of New Hybrid Pyrazole Ligand: Synthesis and Characterization of Several Zn^{II}, Cd^{II}, Hg^{II}, Pd^{II}, Pt^{II}, and Ni^{II} Complexes

Miguel Guerrero,[†] Josefina Pons,*[,†] Teodor Parella,[‡] Mercè Font-Bardia,[§] Teresa Calvet,[§] and Josep Ros*[,†]

[†]*Departament de Química, Unitat de Química Inorgànica and* [‡]*Departament de Química i Servei de RMN and Universitat Autònoma de Barcelona, 08193-Bellaterra, Barcelona, Spain, and* [§]*Cristal·lografia, Mineralogia i Dipòsits Minerals, Universitat de Barcelona, Martí i Franquès s/n, 08028 Barcelona, Spain*

Received May 11, 2009

In this paper we describe the synthesis of the new mixed-donor ligand 1,8-bis(3,5-dimethyl-1*H*-pyrazol-1-yl)-3,6-dioxaoctane (**L**). The complexes $[MCl_2(L)]$ (M=Zn^{II} (**1**), Cd^{II} (**2**), Hg^{II} (**3**), Pd^{II} (**4**), Pt^{II} (**6**), Ni^{II} (**7**)) and $[PdCl_2(L)]_2$ (**5**) were prepared and fully characterized. X-ray crystal structures of complexes **1**, **2**, **4**, **6**, and **7** have been determined. The **L** ligand behaves either as a *NN*-bidentate (chelate or bridge) and *NOON*-tetradentate (equatorial or planar) ligand. In these structures, C−H···X (X=O, N or Cl/Cl^-) intermolecular interactions have been identified and studied. Moreover, the $^{113}Cd\{^1H\}$, $^{195}Pt\{^1H\}$, and $^{199}Hg\{^1H\}$ NMR spectra were measured to investigate the coordination environment of the metal in solution. Diffusion NMR studies have also been performed to characterize monomeric and dimeric species of Pd^{II}. Finally, we have observed that the dimeric complex **5** is converted into the corresponding monomeric complex **4**.

Introduction

The rich diversity of transition metal coordination chemistry provides exciting prospects for the design of novel coordination ligands having unique structures and valuable functional characteristics.[1] Significant efforts directed toward the design of specific architectures formed by the self-assembly processes have been carried out in a number of fields of synthetic chemistry.[2]

The recent past has evidenced an ever-increasing interest in pyrazole-based hybrid ligands. The interest in such compounds is due, first of all, to their variety of coordination complexes with a great number of metal ions and, second, to their ability to provide an extensive variety of coordination geometries and significant structural nuclearity when introducing different kinds of heteroatoms.[3] The past few years have seen a considerable rise in interest in the design of various pyrazole-based ligands as well as the study of their structural properties to serve specific stereochemical requirements for a particular metal-binding site.[4]

The combination of coordination chemistry with intermolecular interactions, such as hydrogen bonding, provides a powerful method for creating supramolecular architectures from simple building blocks. Both types of connection are valuable for the design of network solids since they are directional interactions. The advantage of using transition metal ions is that the shape of the main building block (coordination unit) can be controlled by using organic ligand-bound metal-containing modules in directions dictated by the coordination geometry of the metal center.[5]

In the recent past years, our research group has focused its interest on the synthesis and characterization of heterotopic ligands combining a pyrazolyl group with other donor groups containing S, N, P, and/or O atoms, and in the study

*To whom correspondence should be addressed. E-mail: josefina.pons@uab.es.

(1) (a) Gardner, G. B.; Venkataraman, D.; Moore, J. S.; Lee, S. *Nature* **1995**, *374*, 792–793. (b) Venkataraman, D.; Gardner, G. B.; Lee, S.; Moore, J. S. *J. Am. Chem. Soc.* **1995**, *117*, 11600–11601. (c) Yaghi, O. M.; Li, G.; Li, H. *Nature* **1995**, *378*, 703–706. (d) Hennigar, T. J.; MacQuarrie, D. C.; Losier, P.; Rogers, R. D.; Zaworotko, M. J. *Angew. Chem., Int. Ed. Engl.* **1997**, *36*, 972–973. (e) Vatsadze, S. Z.; Nuriev, V. N.; Zyk, N. V. *Chem. Heterocycl. Compd.* **2005**, *9*, 1091–1101. (f) Kitagawa, S.; Kitaura, R.; Noro, S. *Angew. Chem., Int. Ed.* **2004**, *43*, 2334–2375. (g) Janiak, C. *Dalton Trans.* **2003**, *14*, 2781–2804.

(2) (a) Batten, S. T.; Robson, R. *Angew. Chem., Int. Ed.* **1998**, *37*, 1461–1494. (b) Nguyen, P.; Gomez-Elipe, P.; Manners, I. *Chem. Rev.* **1999**, *99*, 1515–1548. (c) Leininger, S.; Olenyuk, B.; Stang, P. J. *Chem. Rev.* **2000**, *100*, 853–907. (d) Swiegers, G. F.; Malefetse, T. J. *Chem. Rev.* **2000**, *100*, 3483–3537.

(3) (a) Trofimenko, S. *Chem. Rev.* **1993**, *93*, 943–980. (b) Mukherjee, R. *Coord. Chem. Rev.* **2000**, *203*, 151–218. (c) Halcrow, M. A. *Dalton Trans.* **2009**, *12*, 2059–2073.

(4) (a) Halcrow, M. A. *Coord. Chem. Rev.* **2005**, *249*, 2880–2908. (b) Bigmore, H. R.; Lawrence, S. C.; Mountford, P.; Tredget, C. S. *Dalton Trans.* **2005**, *24*, 635–651. (c) Reger, D. L.; Foley, E. A.; Smith, M. D. *Inorg. Chem.* **2009**, *48*, 936–945.

(5) (a) Piguet, C.; Bernardinelli, G.; Hopfgartner, G. *Chem. Rev.* **1997**, *97*, 2005–2062. (b) Desiraju, G. R. *Acc. Chem. Res.* **2002**, *35*, 565–573. (c) Khlobystov, A. N.; Blake, A. J.; Champness, N. R.; Lemenovskii, D. A.; Majouga, G.; Zyk, N. V.; Schroder, M. *Coord. Chem. Rev.* **2001**, *222*, 155–192. (d) Hagrman, P. J.; Hagrman, D.; Zubieta, J. *Angew. Chem., Int. Ed.* **1999**, *38*, 2638–2684. (e) Aakeröy, C. B.; Beatty, A. M. *Aust. J. Chem.* **2001**, *54*, 409–421.

Published on Web 08/19/2009

of their reactivity with several transition metals such as Zn^{II}, Cd^{II}, Pd^{II}, Pt^{II}, Rh^{I}, or Ru^{II}.[6]

The coordination chemistry of the hybrid *N,S*-donor ligands has attracted the attention of several groups.[7] However, the chemistry of the d^8- and d^{10}-configured metals with *N,O*-ligands remains much less developed, but it is potentially interesting because these ligands contain both a soft nitrogen donor site and a hard oxygen donor site. The presence of these disparate sites can lead to aggregation of soft and hard metal centers.[8]

We have recently reported the synthesis and characterization of three new 3,5-dimethylpyrazolic hybrid ligands *N1*-substituted by polyether chains and phenyl groups and studied their reactivity with Pd^{II}.[6j] The aim of this paper is to extend this past work to a new potentially tetradentate *N,O*-hybrid pyrazole ligand and to investigate its variable coordination behavior toward d^8- and d^{10}-configured metals. We now report the results of our investigations into the ligand properties of 1,8-bis(3,5-dimethyl-1*H*-pyrazol-1-yl)-3,6-dioxaoctane (**L**) with Zn^{II} (**1**), Cd^{II} (**2**), Hg^{II} (**3**), Pd^{II} (**4** and **5**), Pt^{II} (**6**), and Ni^{II} (**7**) ions to compare the difference between **L** and the previous reported ligands. We shall describe the X-ray crystal structures, C−H···X (X = O, N or Cl/Cl^-) intermolecular interactions, and the NMR studies of the monomeric, dimeric, and polymeric complexes.

Results and Discussion

Synthesis of the Ligand. The synthetic procedure for the preparation of the **L** ligand, 1,8-bis(3,5-dimethyl-1*H*-pyrazol-1-yl)-3,6-dioxaoctane, consists of two steps (Scheme 1). First, 3,5-dimethylpyrazole was reacted with NaH in dry tetrahydrofuran (THF) to give the corresponding sodium salt. In the second step, 1,2-bis(2-chloroethoxy)ethane was added to the sodium 3,5-dimethylpyrazolate giving rise to the **L** ligand. The ligand has been fully determined and characterized by melting point, elemental analysis, mass spectrometry, and IR, ^1H and $^{13}C\{^1H\}$ NMR spectroscopies. The NMR signals were assigned by reference to the literature[9] and from the analysis of DEPT, COSY, and HMQC spectra. Elemental analysis, mass spectrometry, and all spectroscopic data for **L** are consistent with the proposed structure.

Scheme 1

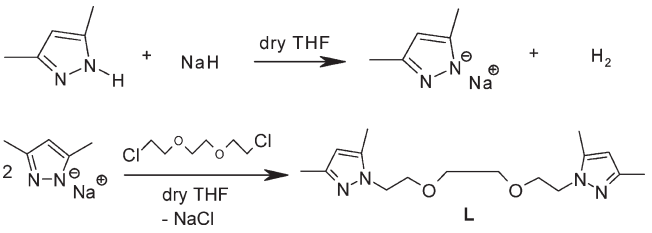

Synthesis and General Characterization of Complexes. The reaction of **L** with MCl_2 (M = Zn^{II}, Cd^{II}, or Hg^{II}) in absolute ethanol for 2 h yields the neutral complexes $[MCl_2(L)]$ [M = Zn^{II} (**1**), Cd^{II} (**2**), Hg^{II} (**3**)]. Moreover, the reaction between **L** ligand and $[PdCl_2(CH_3CN)_2]$[10] gives two types of compounds, monomer and dimer, depending upon the solvent (Scheme 2). Monomeric complex $[PdCl_2(L)]$ (**4**) was obtained by treatment of the **L** ligand with Pd^{II} in CH_3CN for 36 h at 60 °C. On the other hand, dimeric complex $[PdCl_2(L)]_2$ (**5**) was obtained by treatment of the **L** ligand with Pd^{II} in THF or CH_2Cl_2 for 12 h at RT. Furthermore, the corresponding DOSY spectra indicate the existence of two different-sized species that strongly agree with the existence of the monomeric and dimeric complexes. The reaction of **L** and K_2PtCl_4 in distilled H_2O for 2 h yields the complex $[PtCl_2(L)]$ (**6**). Finally, when the **L** ligand reacts with $NiCl_2 \cdot 6H_2O$ in absolute ethanol for 24 h complex $[NiCl_2(L)]$ (**7**) is obtained. This complex is highly hygroscopic. All the reactions were carried out in a 1:1 M/L molar ratio.

Several techniques were used for the characterization of all complexes: elemental analyses, mass spectrometry, conductivity measurements, IR, and 1D and 2D NMR spectroscopies. In addition a full three-dimensional structure determination for compounds **1**, **2**, **4**, **6**, and **7** was performed. In the case of compounds **3** and **5** regretfully no suitable single crystals could be obtained.

The elemental analyses for complexes **1**−**7** are consistent with the formula $[MCl_2(L)]$ [M = Zn^{II} (**1**), Cd^{II} (**2**), Hg^{II} (**3**), Pd^{II} (**4** and **5**), Pt^{II} (**6**), and Ni^{II} (**7**)]. The positive ionization spectra (ESI^+-MS) of compounds **1**−**4** and **7** give a peak attributable to $[MCl(L)]^+$. For compound **5** a peak attributable to $[M_2Cl_3(L)]^+$ is observed because of the dimeric nature of this compound, and for compound **6**, the molecular peak is attributable to $[MCl_2(L)+Na]^+$. Molecular peaks of the cations are observed with the

(6) (a) Aragay, G.; Pons, J.; García-Antón, J.; Solans, X.; Font-Bardia, M.; Ros, J. *J. Organomet. Chem.* **2008**, *693*, 3396–3404. (b) Montoya, V.; Pons, J.; Branchadell, V.; García-Antón, J.; Solans, X.; Font-Bardia, M.; Ros, J. *Organometallics* **2008**, *27*, 1084–1091. (c) Muñoz, S.; Pons, J.; Solans, X.; Font-Bardia, M.; Ros, J. *J. Organomet. Chem.* **2008**, *693*, 2132–2138. (d) de León, A.; Pons, J.; García-Antón, J.; Solans, X.; Font-Bardia, M.; Ros, J. *Polyhedron* **2007**, *26*, 2921–2928. (e) Montoya, V.; Pons, J.; García-Antón, J.; Solans, X.; Font-Bardia, M.; Ros, J. *Organometallics* **2007**, *26*, 3183–3190. (f) Pañella, A.; Pons, J.; García-Antón, J.; Solans, X.; Font-Bardia, M.; Ros, J. *Inorg. Chim. Acta* **2006**, *359*, 4477–4482. (g) Tribó, R.; Muñoz, S.; Pons, J.; Yáñez, R.; Larena, A. A.; Piniella, J. F.; Ros, J. *J. Organomet. Chem.* **2005**, *690*, 4072–4079. (h) García-Antón, J.; Pons, J.; Solans, X.; Font-Bardia, M.; Ros, J. *Eur. J. Inorg. Chem.* **2003**, *16*, 2992–3000. (i) Esquius, G.; Pons, J.; Yáñez, R.; Ros, J.; Mathieu, R.; Lugan, N.; Donnadieu, B. *J. Organomet. Chem.* **2003**, *667*, 126–134. (j) Guerrero, M.; Pons, J.; Branchadell, V.; Parella, T.; Solans, X.; Font-Bardia, M.; Ros, J. *Inorg. Chem.* **2008**, *23*, 11084–11094. (k) Pons, J.; García-Antón, J.; Jimenez, R.; Solans, X.; Font-Bardia, M.; Ros, J. *Inorg. Chem. Commun.* **2007**, *10*, 1554–1556. (l) de León, A.; Pons, J.; García-Antón, J.; Solans, X.; Font-Bardia, M.; Ros, J. *Polyhedron* **2007**, *26*, 2498–2506.

(7) (a) Braunstein, P.; Naud, F. *Angew. Chem., Int. Ed.* **2001**, *40*, 680–699. (b) Slone, C. S.; Weinberger, D. A.; Mirkin, C. A. *Prog. Inorg. Chem.* **1999**, *48*, 233–350. (c) Bader, A.; Lindner, E. *Coord. Chem. Rev.* **1991**, *108*, 27–110. (d) Boog-Wick, K.; Pregosin, P. S.; Trabesinger, G. *Organometallics* **1998**, *17*, 3254–3264. (e) Sinha, C.; Bandyopadhyay, D.; Chakravorty, A. *Inorg. Chem.* **1998**, *27*, 1173–1178. (f) Chelucci, G.; Muroni, D.; Saba, A.; Saccolini, F. *J. Mol. Catal. A. Chem.* **2003**, *197*, 27–35. (g) Stibrany, R. T.; Fox, S.; Bharadwaj, P. K.; Schugar, H. J.; Potenza, J. A. *Inorg. Chem.* **2005**, *44*, 8234–8242. (h) Tresoldi, G.; Baradello, L.; Lanza, S.; Cardiano, P. *Eur. J. Inorg. Chem.* **2005**, *12*, 2423–2434. (i) Raper, E. S. *Coord. Chem. Rev.* **1997**, *165*, 475–567. (j) Krebs, B.; Henkel, G. *Angew. Chem., Int. Ed. Engl.* **1991**, *30*, 769–788. (k) Hardt, S.; Schollmeyer, D.; Fleischer, H. *Inorg. Chem.* **2006**, *45*, 8318–8325. (l) Sousa-Pedrares, A.; Romero, J.; Garcia-Vazquez, J. A.; Duran, M.; Casanova, I. *Dalton Trans.* **2003**, *7*, 1379–1388. (m) Englich, U.; Ruhland-Senge, K. *Coord. Chem. Rev.* **2000**, *210*, 135–179.

(8) (a) Würthner, F.; You, C.; Saha-Möller, C. R. *Chem. Soc. Rev.* **2004**, *33*, 133–146. (b) Fallis, I. A. *Annu. Rep. Prog. Chem., Sect. A* **1999**, *95*, 313–351. (c) Steel, P. J. *Molecules* **2004**, *9*, 440–448. (d) Ward, M. D. *Annu. Rep. Prog. Chem., Sect. A* **1999**, *95*, 261–312.

(9) (a) Pretsh, E.; Clerc, T.; Seibl, J.; Simon W. *Tables of Determination of Organic Compounds. 13C NMR, 1H NMR, IR, MS, UV/Vis, Chemical Laboratory Practice*; Springer-Verlag: Berlin, 1989. (b) Williams, D. H.; Fleming, I. *Spectroscopic Methods in Organic Chemistry*; McGraw-Hill: London, 1995.

(10) Komiya, S. *Synthesis of Organometallic Compounds: A Practice Guide*; Board: New York, 1997.

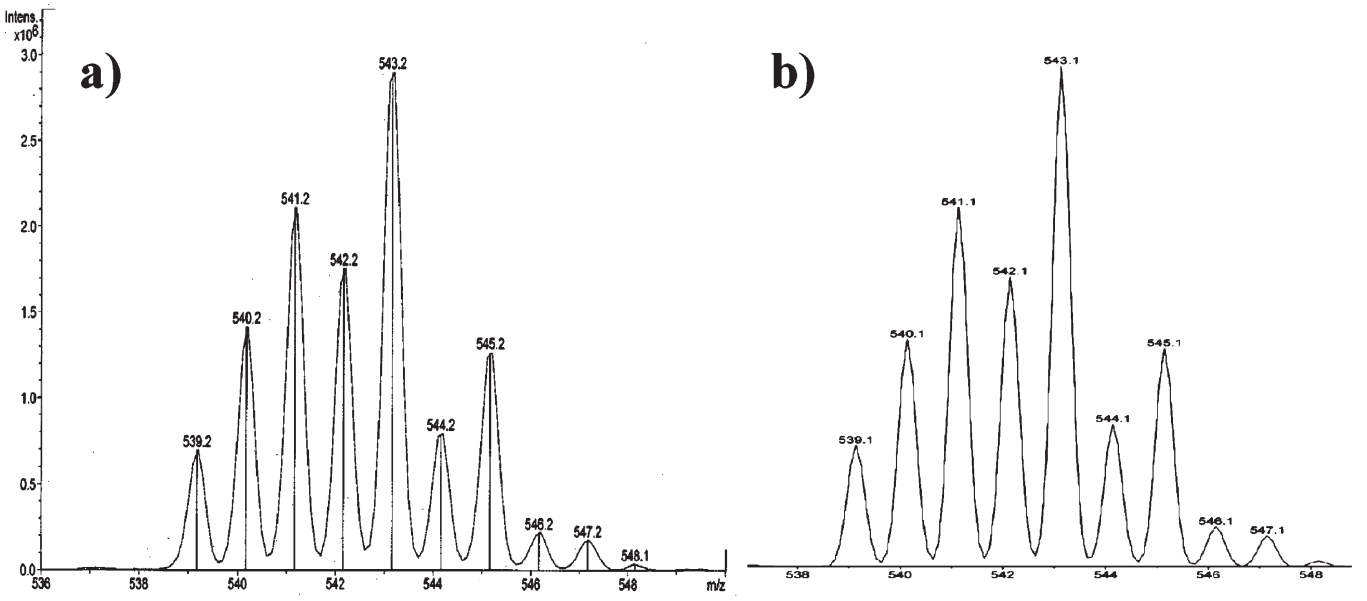

Figure 1. (a) ESI^+-MS spectra in methanol of fragment $[HgCl(\mathbf{L})]^+$ for complex **3** and (b) theoretical isotopic distribution of **3**.

Scheme 2

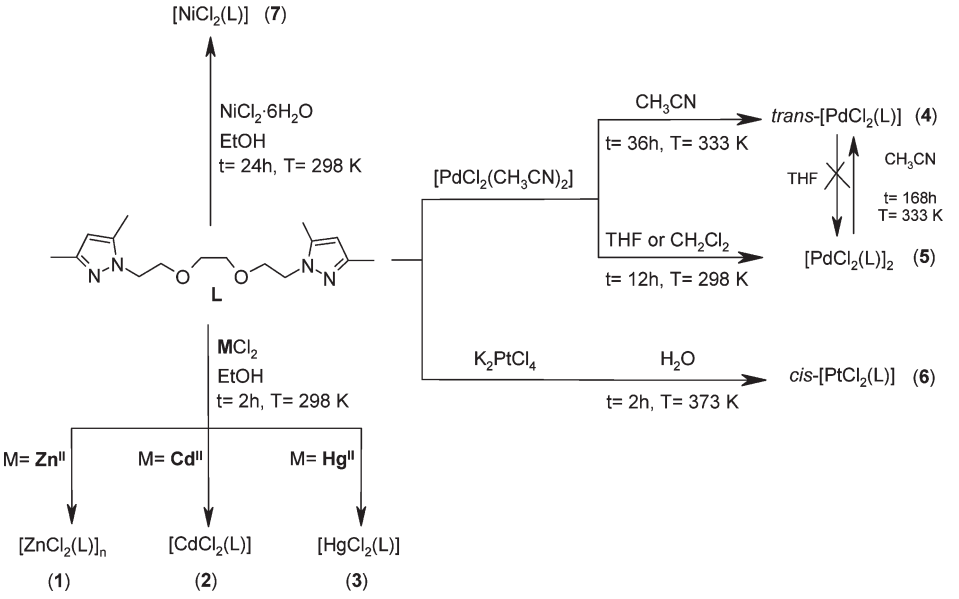

same isotope distribution as the theoretical ones. As an example, ESI^+-MS spectra of complex **3** for fragment $[HgCl(L)]^+$ and its theoretical isotopic distribution is presented (Figure 1).

Conductivity values in methanol for complexes **1**−**6** are in agreement with the presence of non-electrolyte compounds since reported values (21.4−37.2 S cm^2 mol^{-1}) are lower than 80 S cm^2 mol^{-1}. However, the conductivity value of complex **7** in methanol (187.0 S cm^2 mol^{-1}) is in agreement with a 1:2 electrolyte (tabulated values are between 160 and 220 S cm^2 mol^{-1}) whereas the conductivity value in acetone (29.5 S cm^2 mol^{-1}) is in agreement with a non-electrolyte complex (reported values are lower than 100 S cm^2 mol^{-1}).[11]

Therefore, the electronic spectrum of complex **7** was recorded in these two different solvents to study the geometry of the complex in solution. The spectrum, recorded in methanol, exhibits two bands in the visible region, at 677 and 581 nm ($\varepsilon = 12$ and 17 mol^{-1} cm^{-1} L, respectively). In acetone, the spectrum also shows two bands at 681 and 595 nm ($\varepsilon = 13$ and 21 mol^{-1} cm^{-1} L, respectively). All these bands are characteristic of octahedral Ni^{II} complexes.[12] So, the local environment in methanol around Ni^{II} is $[NiN_2O_4]^{2+}$ with two non-coordinate chloride anions (**7′**) whereas in acetone, the two chlorine atoms are coordinated to the metallic center $[NiN_2O_2Cl_2]$ (**7**).

(11) (a) Geary, W. J. *Coord. Chem. Rev.* **1971**, *7*, 81–122. (b) Thompson, L. K.; Lee, F. L.; Gabe, E. J. *Inorg. Chem.* **1988**, *27*, 39–46.

(12) (a) Sutton, D. *Electronic Spectra of Transition Metal Complexes*; McGraw-Hill: London, 1975. (b) Cotton, F. A.; Wilkinson, G. *Advanced Inorganic Chemistry*; 5th ed.; Wiley: New York, 1988.

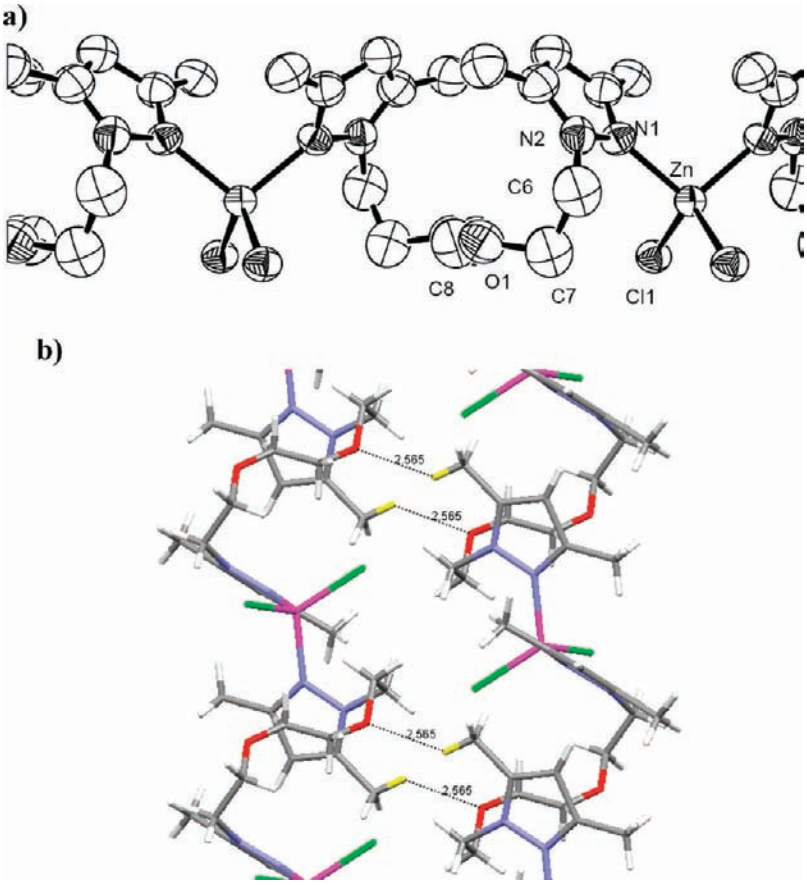

Figure 2. (a) Oak Ridge thermal ellipsoid plot (ORTEP) diagram of complex **1** showing an atom labeling scheme. 50% probability amplitude displacement ellipsoids are shown. Hydrogen atoms are omitted for clarity. See Table 1 for selected values of the bond lengths and bond angles. (b) View of some bonding interactions in the crystal structure.

The IR spectra of complexes **1**−**7** in the range 4000−400 cm^{-1} show that the **L** ligand is coordinated to the metallic center. The most characteristic bands in the IR spectra are those attributable to the pyrazolyl and ether groups.[9] The IR spectra of complexes **1**−**7** in the 600−100 cm^{-1} region were also studied. The presence of bands between 512 and 478 cm^{-1}, for all complexes, assigned to ν(M−N) confirms the coordination of the N_{pz} of the ligand to the metallic atom. It is remarkable to note that complexes **4** and **5** display a ν(Pd−Cl) single band between 352 and 347 cm^{-1}. This band indicates that the chlorine atoms are coordinated to Pd^{II} in *trans* disposition. In contrast, complex **6** displays two ν(Pt−Cl) bands at 340 and 328 cm^{-1}, indicating that the chlorine atoms are coordinated to the Pt^{II} atom in *cis* disposition.[13]

Crystal Structures of Complexes 1 and 2. For complexes **1** and **2**, it has been possible to obtain colorless monocrystals suitable for X-ray analyses through crystallization from a diethyl ether/dichloromethane (1:1) mixture. Despite their analogous constitution, $[MCl_2(L)]$, the zinc (**1**) and the cadmium (**2**) compounds display different coordination modes to the metal ion. Complex **1** (Figure 2a) has a polymeric structure and shows a one-dimensional infinite neutral chain $[ZnCl_2(L)]_n$ wherein the ligand **L** bridges adjacent tetrahedral metal centers. The local coordination environment around Zn(II) atom is formed by two pyrazolyl nitrogen atoms and two chlorines. The coordination sphere of Zn^{II} can be described as a slightly distorted tetrahedral geometry with angles between 100.10(15) and 117.67(7)°. The $[ZnCl_2(N_{pz})_2]$ *core* is present in 18 complexes in the literature[14] but none of them present a polymeric structure. Selected values of bond lengths and bond angles for complex **1** are shown in Table 1. The Zn−Cl and Zn−N_{pz} bond distances are in

Table 1. Selected Bond Lengths (Å) and Bond Angles (deg) for **1** and **2**

	1 (Zn^{II})	**2** (Cd^{II})
M−N (1)	2.045(3)	2.3111(19)
M−N (4)	2.045(3)	2.3111(19)
M−Cl (2)	2.2574(15)	2.5090(8)
M−Cl (1)	2.2574(15)	2.5090(8)
M−O (1)		2.6581(13)
N (1)−M−N (4)	100.10(15)	144.76(8)
N (1)−M−Cl (2)	117.67(7)	99.47(5)
N (4)−M−Cl (2)	104.32(8)	103.12(5)
N (1)−M−Cl (1)	104.32(8)	103.12(5)
N (4)−M−Cl (1)	117.67(7)	99.47(5)
Cl (2)−M−Cl (1)	112.69(7)	99.39(4)
N (4)−M−O (1)		73.78(4)
N (4)−M−O (2)		76.71(5)
Cl (2)−M−O (1)		96.99(3)
Cl (2)−M−O (2)		163.61(4)
O (2)−M−O (1)		66.62(3)

(13) Nakamoto, K. *Infrared and Raman Spectra of Inorganic and Coordination Compounds*; John Wiley and Sons: New York, 1986.

(14) Allen, F. A. *Acta Crystallogr.* **2002**, *B58*, 380–388.

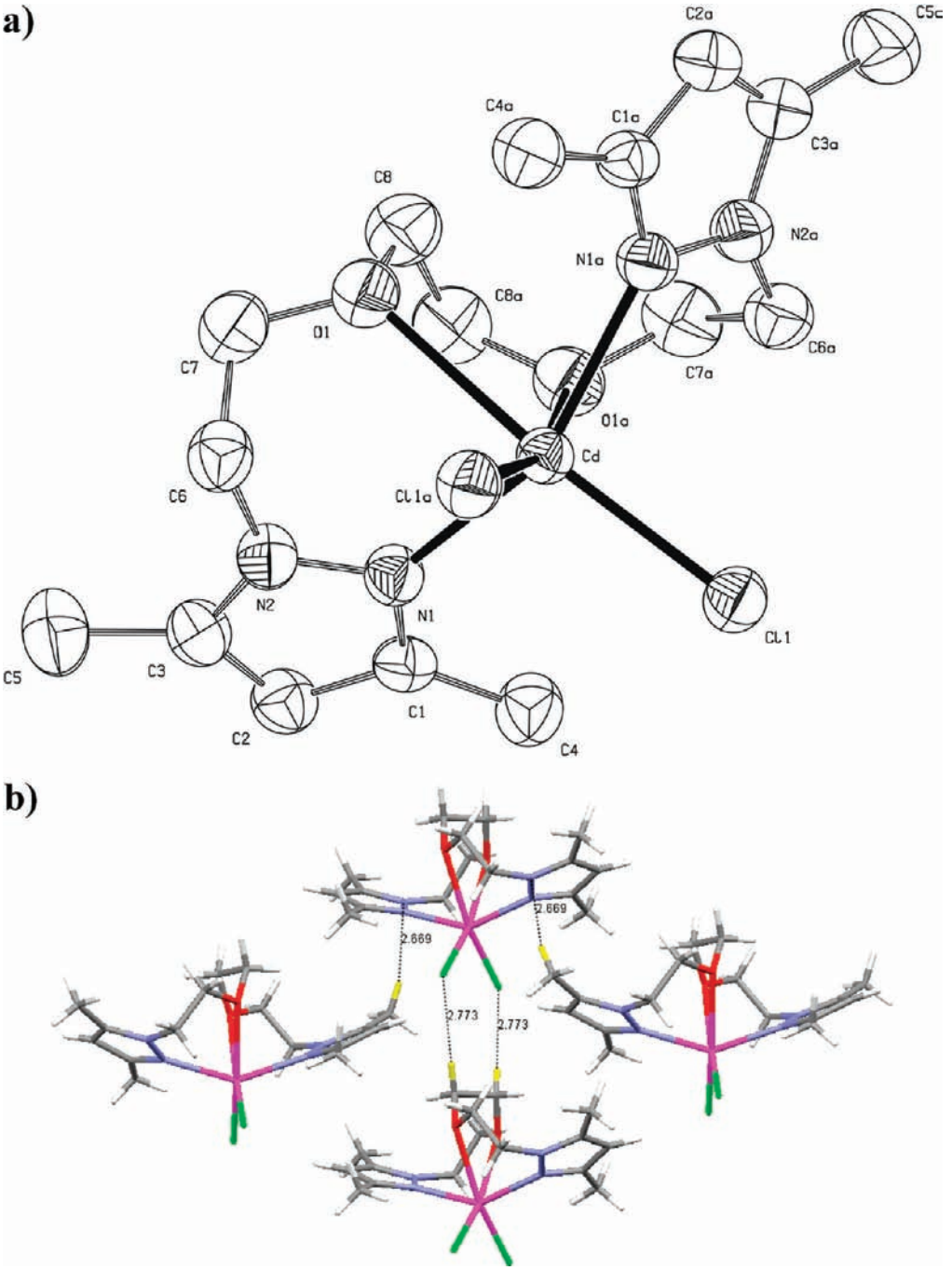

Figure 3. (a) ORTEP diagram of complex **2** showing an atom labeling scheme. 50% probability amplitude displacement ellipsoids are shown. Hydrogen atoms are omitted for clarity. See Table 1 for selected values of the bond lengths and bond angles. (b) View of some bonding interactions in the crystal structure.

agreement with the values reported in the literature (2.188−2.373 Å and 1.945−2.172 Å, respectively),[15] and the N−Zn−N and Cl−Zn−Cl angles are within the expected range for zinc(II) compounds with a tetrahedral geometry. In the crystal structure of **1**, Zn^{II} metal centers are connected to each other by **L** ligand through a *NN*-bidentate bridging mode into a 1D chain along the crystallographic *a*-direction, in which the distance between adjacent Zn atoms is 9.523 Å.

In contrast, the structure of complex **2** (M = Cd^{II}) consists of discrete neutral monomeric units (Figure 3a). The cadmium atom is coordinated to two *cis* chlorine atoms, two *trans* pyrazolic nitrogen atoms, and two *cis* ether oxygen atoms. The **L** ligand in complex **2** is coordinated to the metal centers in a κ^4 *NOON*-bonding mode. The **L** ligand chelates the center metal atoms through the pyrazolic nitrogen atoms and the ether oxygen atoms to form two six-membered rings and one five-membered ring. The metal center, which adopts distorted

(15) (a) Balamurugan, V.; Hundal, M. S.; Mukherjee, R. *Chem.—Eur. J.* **2004**, *10*, 1683–1690. (b) Schuitema, A. M.; Engelen, M.; Koval, I. A.; Gorter, S.; Driessen, W. L.; Reedijk, J. *Inorg. Chim. Acta* **2001**, *324*, 57–64. (c) Luo, Y.; Potvin, P. G. *J. Coord. Chem.* **1999**, *46*, 319–344. (d) Bieller, S.; Bolte, M.; Lerner, H. W.; Wagner, M. *J. Organomet. Chem.* **2005**, *690*, 1935–1946.

octahedral coordination geometry, shows bond angles between 99.39° and 144.76°. These angles significantly deviate from 90° or 180°, presumably because of the restrictions provoked by the chelation of the tetradentate **L** ligand. The $[CdCl_2(N_{pz})_2O_2]$ *core* is not present in the literature[14] but the $[CdCl_2N_2O_2]$ *core* is present in five complexes in the literature.[16] As seen in Table 1, the Cd−O distances (2.658(2) Å) are significantly longer than the Cd−N distances (2.3111(19) Å). The numbers of parameters refined and other details concerning the refinement of the crystal structures **1** and **2** are gathered in Table 3.

In the literature it is observed that there are significant differences between the tetrahedral/octahedral geometry with Zn^{II} and Cd^{II} (both cations are d^{10}-configured metals). When Zn^{II} is used the preferred geometry is tetrahedral (**67/33**) whereas the octahedral geometry is the most common when the metallic center is Cd^{II} (**34/66**). Generally, it is attributed to the different atoms' size (ionic radius: 74 ppm (Zn^{II}) and 97 ppm (Cd^{II})).[14,17]

Crystal Structures of Complexes 4 and 6. For complexes **4** and **6**, it has been possible to obtain pale yellow monocrystals suitable for X-ray analyses through crystallization from a diethyl ether/dichloromethane (1:1) mixture (**4**) and from THF/dichloromethane (1:1) mixture (**6**). Contrary to what we have found for complexes **1** and **2**, **L** ligand acts in complexes **4** and **6** as a *NN*-bidentate chelate ligand and forms two metallocyles with square planar geometry where the oxygen atoms of the chain remain non-coordinated to metal. This kind of coordination is similar to $[PdCl_2(L_A)]$ (L_A = 1,2-bis[4-(3,5-dimethyl-1*H*-pyrazol-1-yl)-2-oxabutyl]benzene) (**4A**), recently published by our group.[6j] The ether moieties can enter into non-covalent interactions and also control the covalent bonding by altering the directional orientation of the pyrazole units.[18]

The molecular structure of complex **4** (Figure 4a) consists of Pd(II) discrete molecules with a very slightly distorted square planar geometry around the metal atom and one solvent molecule severely disordered of diethyl ether. The environment consists of two chlorine atoms in *trans* disposition to the Pd(II) and two nitrogen atoms of the pyrazolic rings of **L**. The N(1)−Pd−N(4) and Cl(1)−Pd−Cl(2) bond angles values are 177.77(7)° and 179.17(3)°, respectively, showing a slightly tetrahedral distortion. This distortion in complex **4** can also be observed from the deviation (0.009 Å) of the Pd^{II} from the mean plane (N(1), N(4), Cl(1), Cl(2)). In comparison with the distortion of the complex **4A** (0.085 Å),[6j] it seems that the new ligand (**L**) is a more flexible derivate ligand because of its deviation is significantly smaller. The **L** ligand acts as a bidentate chelate and forms a metallacycle ring of 13 members. The $[PdCl_2(N_{pz})_2]$ *core*, with a bidentate chelate ligand, is present in 13 complexes described in the literature.[14] Only two of these structures present the chlorine atoms in *trans* disposition.[6j,19] Selected values of bond lengths and bond angles for complex **4** are shown in Table 2. The Pd−Cl and Pd−N_{pz} bond distances are in agreement with the values reported in the literature (2.220−2.361 Å and 1.979−2.141 Å, respectively),[19,20] and the N−Pd−N and Cl−Pd−Cl angles are also consistent with the values found in the literature for palladium compounds with a distorted square planar geometry.[14]

Table 2. Selected Bond Lengths (Å) and Bond Angles (deg) for **4**, **6**, and **7′**

	4 (Pd^{II})	**6** (Pt^{II})	**7′** (Ni^{II})
M−N (1)	2.006(2)	2.040(4)	2.071(2)
M−N (4)	2.022(2)	2.023(3)	2.087(2)
M−Cl (2)	2.3125(10)	2.3142(13)	
M−Cl (1)	2.3130(10)	2.3001(13)	
M−O (1)			2.101(2)
M−O (2)			2.092(2)
M−O (3)			2.052(2)
M−O (4)			2.063(2)
N (1)−M−N (4)	177.77(7)	96.59(13)	107.38 (8)
N (1)−M−Cl (2)	88.28(6)	87.71(10)	
N (4)−M−Cl (2)	90.70(6)	174.59(10)	
N (1)−M−Cl (1)	91.60(6)	176.59(9)	
N (4)−M−Cl (1)	89.45(6)	85.77(10)	
Cl (2)−M−Cl (1)	179.17(3)	90.09(5)	
N (4)−M−O (1)			161.57(8)
N (4)−M−O (2)			90.14(9)
O (4)−M−O (1)			92.75(8)
O (4)−M−O (2)			82.30(9)
O (2)−M−O (1)			75.38(9)
N (1)−M−O (4)			89.43(9)
N (4)−M−O (4)			96.59(9)
N (1)−M−O (3)			94.81(9)
N (4)−M−O (3)			84.71(8)
O (4)−M−O (3)			175.00(9)

The crystal structure of complex **6** consists of monomeric *cis*-$[PtCl_2(L)]$ molecules (Figure 5a) and one solvent molecule of THF. The environment consists of two chlorine atoms and two nitrogen atoms of the pyrazolic rings. The platinum center has a square planar geometry with a slight tetrahedral distortion and similar deviation from the mean plane (0.008 Å) as Pd^{II} (**4**). The main difference between complexes **4** and **6** relies on the disposition of the chlorine atoms: in complex **4** the two chlorines are in *trans* disposition whereas in complex **6** the two chlorines are in *cis* disposition. This difference in the

(16) (a) Gagnon, C.; Beauchamp, A. L.; Tranqui, D. *Can. J. Chem.* **1979**, *57*, 1372–1376. (b) Xue, X.; Wang, X.; Wang, L.; Xiong, R.; Abrahams, B.; You, X.; Xue, Z.; Che, C. *Inorg. Chem.* **2002**, *41*, 6544–6546. (c) Odoko, M.; Isomoto, N.; Okabe, N. *Acta Crystallogr., Sect. E: Struct. Rep. Online* **2001**, *57*, m371–m372. (d) Li, M.; Yan, L.; Wang, J.; Zhou, J. *Acta Crystallogr., Sect. E: Struct. Rep. Online* **2006**, *62*, m2517–m2518. (e) Yeh, C.; Hu, H.; Liang, R.; Wang, K.; Yen, T.; Chen, J.; Wang, J. *Polyhedron* **2005**, *24*, 539–548.

(17) (a) Greenwood, N. N.; Earmshow, A. *Chemistry of the Elements*; Butterworth-Heinenmann: Oxford, 1997. (b) Housecroft, C. E.; Sharpe, A. G. *Inorganic Chemistry*; Prentice Hall: London, 2001.

(18) (a) Holliday, B. J.; Ulmann, P. A.; Mirkin, C. A.; Stern, C. L. *Organometallics* **2004**, *23*, 1671–1679. (b) Masar, M. S., III; Ovchinnikov, M. V.; Mirkin, C. A.; Zakharov, L. V.; Rheingold, A. L. *Inorg. Chem.* **2003**, *42*, 6851–6858. (c) Brown, A. M.; Ovchinnikov, M. V.; Stern, C. L.; Mirkin, C. A. *J. Am. Chem. Soc.* **2004**, *126*, 14316–14317. (d) Gianneschi, N. C.; Masar, M. S., III; Mirkin, C. A. *Acc. Chem. Res.* **2005**, *11*, 825–837. (e) Redshaw, C. *Coord. Chem. Rev.* **2003**, *244*, 45–70. (f) Dawe, L. N.; Abedine, T. S.; Thompson, L. K. *Dalton Trans.* **2008**, *13*, 1661–1675.

(19) García-Antón, J.; Pons, J.; Solans, X.; Font-Bardia, M.; Ros, J. *Eur. J. Inorg. Chem.* **2002**, 3319–3327.

(20) (a) García-Antón, J.; Pons, J.; Solans, X.; Font-Bardia, M.; Ros, J. *Inorg. Chim. Acta* **2003**, *355*, 87–94. (b) Boixassa, A.; Pons, J.; Solans, X.; Font-Bardia, M.; Ros, J. *Inorg. Chim. Acta* **2003**, *346*, 151–157. (c) Boixassa, A.; Pons, J.; Solans, X.; Font-Bardia, M.; Ros, J. *Inorg. Chim. Acta* **2004**, *357*, 733–738. (d) Torralba, M. C.; Cano, M.; Campo, J. A.; Heras, J. V.; Pinilla, E. *Z. Kristallogr. − New Cryst. Struct.* **2005**, *220*, 617–619. (e) Montoya, V.; Pons, J.; Solans, X.; Font-Bardia, M.; Ros, J. *Inorg. Chim. Acta* **2006**, *359*, 25–34. (f) Spencer, L. C.; Guzei, I. A.; Ojwach, S. O.; Darkwa, J. *Acta Crystallogr., Sect. C: Cryst. Struct. Commun.* **2006**, *62*, m421–m423.

Table 3. Crystallographic Data for **1** and **2**

	1 (Zn^{II})	**2** (Cd^{II})
molecular formula	$C_{16}H_{26}Cl_2N_4O_2Zn$	$C_{16}H_{26}Cl_2N_4O_2Cd$
formula weigh	442.68	489.71
temperature (K)	293(2)	293(2)
wavelength (Å)	0.71073	0.71073
system, space group	orthorhombic, *Pbcn*	orthorhombic, *Pcan*
unit cell dimensions		
a (Å)	9.523 (6)	8.446 (3)
b (Å)	14.924 (11)	14.659 (3)
c (Å)	14.435 (14)	16.235 (5)
α (deg)	90	90
β (deg)	90	90
γ (deg)	90	90
U (Å^3)	2052 (3)	2010.1 (10)
Z	4	4
D_{calc} (g cm^{-3})	1.433	1.618
μ (mm^{-1})	1.474	1.369
F(000)	920	992
crystal size (mm^3)	0.09 × 0.08 × 0.07	0.2 × 0.1 × 0.1
hkl ranges	$-14 \le h \le 12$, $-20 \le k \le 19$, $-22 \le l \le 22$	$-10 \le h \le 10$, $-18 \le k \le 18$, $-18 \le l \le 18$
2θ range (deg)	2.73 to 32.51	2.87 to 30.23
reflections collected/ unique/ [R_{int}]	24866/3577 [R(int) = 0.0358]	14224/2204 [R(int) = 0.0399]
completeness to θ	98.5% (θ = 25.00°)	95.6% (θ = 25.00°)
absorption correction	empirical	empirical
data/restrains/ parameters	3557/10/104	2204/4/116
goodness-of-fit on F^2	0.729	1.328
final R indices [$I > 2\sigma(I)$]	R1 = 0.0403, wR_2 = 0.0866	R1 = 0.0618, wR_2 = 0.1318
R indices (all data)	R1 = 0.1336, wR_2 = 0.0977	R1 = 0.0624, wR_2 = 0.1325
largest diff. peak and hole (e Å^{-3})	0.581 and −1.090	0.995 and −0.877

disposition of the chlorine atoms between Pd^{II} and Pt^{II} complexes with similar ligands had already been observed in the literature[14] and, generally, it is explained by the considerable higher lability of the Pd^{II} compared to Pt^{II}.[21] The *cis*-[$PtCl_2(N_{pz})_2$] *core* is present in eight complexes in the literature[22] but only one of them presents a bidentate chelate ligand, namely, the complex *cis*-[$PtCl_2(L_1)$] (L_1 = bis[2-(3,5-dimethyl-1*H*-pyrazol-1-yl)ethyl]ether).[22b] The Pt−Cl bond distances (2.3001(13) and 2.3142(13) Å), are typical of platinum square-planar complexes, between 2.276(3) and 2.313(2) Å.[14] However, the Pt− N_{pz} (2.040(4) and 2.023(3) Å) bond lengths are the longest reported so far (Pt−N_{pz} distances found in the literature are between 1.935(4) and 2.032(8) Å).[22] All the platinum complexes mentioned above have a *cis* disposition of the pyrazolic ligands. Therefore, angles N−Pt−N and Cl−Pt−Cl are also likely to be compared. In most of the cases, the Cl−Pt−Cl angle appears to be wider than the N−Pt−N angle, often by more than 2°.[22] However, in structure **6**, the angle that is clearly wider is the *bite* angle N−Pt−N and deviate by almost 6°. Other selected values of bond lengths and angle data are gathered in Table 2. As it is observed for complex **4**, the metallic center does not interact with the oxygen atom of the ether group in complex **6** (Pt···O = 4.074(2) and 5.089(2) Å). Thus, the **L** ligand adopts a κ^2 *NN*- bonding mode in **4** and **6**. In this way, this effect can also be used in the future to introduce other hard metallic centers thereby increasing the functionality of the **L** ligand.[18] The numbers of parameters refined and other details concerning the refinement of the crystal structure are gathered in Table 4.

Crystal Structures of Complex 7′. Green suitable crystals for X-ray diffraction experiments of complex [$Ni(H_2O)_2(L)$]Cl_2 (**7′**) were obtained through crystallization from a THF/dichloromethane (1:1) mixture of complex **7**. X-ray analysis indicates that, contrary to what we have found for the other complexes, **7′** is an ionic compound. The crystal structure consists of [$Ni(H_2O)_2(L)$]$^{2+}$ cations and two chloride anions (Figure 6a). In the cation, the nickel atom is coordinated to two pyrazolic nitrogen atoms and two ether oxygen atoms, and the remaining two axial coordination sites are occupied by two water molecules. Pyrazolyl and ether moieties are in *cis* disposition. In the same way as in **2**, the **L** ligand in complex **7′** is coordinated in a κ^4 *NOON*- bonding mode but with a planar disposition in the equatorial plane of the metal cation.

The metal center, which adopts distorted octahedral coordination geometry, has bond angles which vary from 75.38° to 175.00°. These angles significantly deviate from 90° or 180°, respectively. The [$Ni(N_{pz})_2O_4$] *core* is present in 12 structures in the literature[14] but the [$Ni(N_{pz})_2O_2(H_2O)_2$] *core* is only present in 3 complexes in the literature.[23] As seen in Table 2, the Ni−O distances (2.054(2)-2.101(2) Å) are of the same order as the Ni−N distances (2.072(2)−2.087(2) Å) and are similar to other values described in the literature.[23] The numbers of parameters refined and other details concerning the refinement of the crystal structure are gathered in Table 4. In addition, the cations are linked by four O−H···Cl hydrogen bonds. Each chloride anion is involved in two hydrogen bonds (Table 5) forming bridges between coordinated water molecules. This pattern shows infinite chains parallel to the crystallographic vector *c* (Figure 6c).

Extended Structures. We have also studied the extended structures of complexes **1**, **2**, **4**, **6**, and **7'**. In addition to the commonly occurring C−H···N/O/S hydrogen-bonding interactions, the existence of C−H···Cl hydrogen bonds, in general, and charge-assisted (for strengthening noncovalent forces) terminal M−Cl bonds of chlorometalate

(21) (a) Boixassa, A.; Pons, J.; Solans, X.; Font-Bardia, M.; Ros, J. *Inorg. Chim. Acta* **2003**, *355*, 254–263. (b) Boixassa, A.; Pons, J.; Virgili, A.; Solans, X.; Font-Bardia, M.; Ros, J. *Inorg. Chim. Acta* **2002**, *340*, 49–55. (c) Palkin, V. A.; Kuzina, T. A.; Kuzmina, N. N.; Shchelokov, R. N. *Russ. J. Inorg. Chem.* **1980**, *25*, 573–578. (d) Vögtle, F. *Supramolecular Chemistry*; John Wiley and Sons: Chichester, 1991. (e) Wilkinson, G. *Comprehensive Coordination Chemistry: The Synthesis, Reactions, Properties, and Applications of Coordination Compounds, vol 5, Late Transition Elements*; Pergamon Press: Oxford, 1987.

(22) (a) Cafeo, G.; Garozzo, D.; Kohnke, F. H.; Pappalardo, S.; Parisi, M. F.; Nascone, R. P.; Williams, D. J. *Tetrahedron* **2004**, *60*, 1895–1902. (b) Boixassa, A.; Pons, J.; Solans, X.; Font-Bardia, M.; Ros, J. *Inorg. Chim. Acta* **2004**, *357*, 827–833. (c) Raptis, R. G.; Fackler, J. P. *Acta Crystallogr., Sect. C: Cryst. Struct. Commun.* **1991**, *47*, 1180–1183. (d) Broomhead, J. A.; Rendina, L. M.; Sterns, M. *Inorg. Chem.* **1992**, *31*, 1880–1889. (e) Boixassa, A.; Pons, J.; Solans, X.; Font-Bardia, M.; Ros, J. *Inorg. Chim. Acta* **2003**, *355*, 254–263. (f) Cinellu, M. A.; Stoccoro, S.; Minghetti, G.; Bandini, A. L.; Banditelli, G.; Bovio, B. *J. Organomet. Chem.* **1989**, *372*, 311–325. (g) Khripun, A. V.; Selivanov, S. I.; Kukushkin, V. Y.; Haukka, M. *Inorg. Chim. Acta* **2006**, *359*, 320–326. (h) Sakai, K.; Tomita, Y.; Ue, T.; Goshima, K.; Ohminato, M.; Tsubomura, T.; Matsumoto, K.; Ohmura, K.; Kawakami, K. *Inorg. Chim. Acta* **2000**, *297*, 64–71.

(23) (a) Hänggi, G.; Schmalle, H.; Dubler, E. *Inorg. Chem.* **1988**, *27*, 3131–3137. (b) Pan, L.; Ching, N.; Huang, X.; Li, J. *Chem. Eur. J.* **2001**, *20*, 4431–4437. (c) King, P.; Clérac, R.; Anson, C. E.; Powell, A. K. *Dalton Trans.* **2004**, *31*, 852–861.

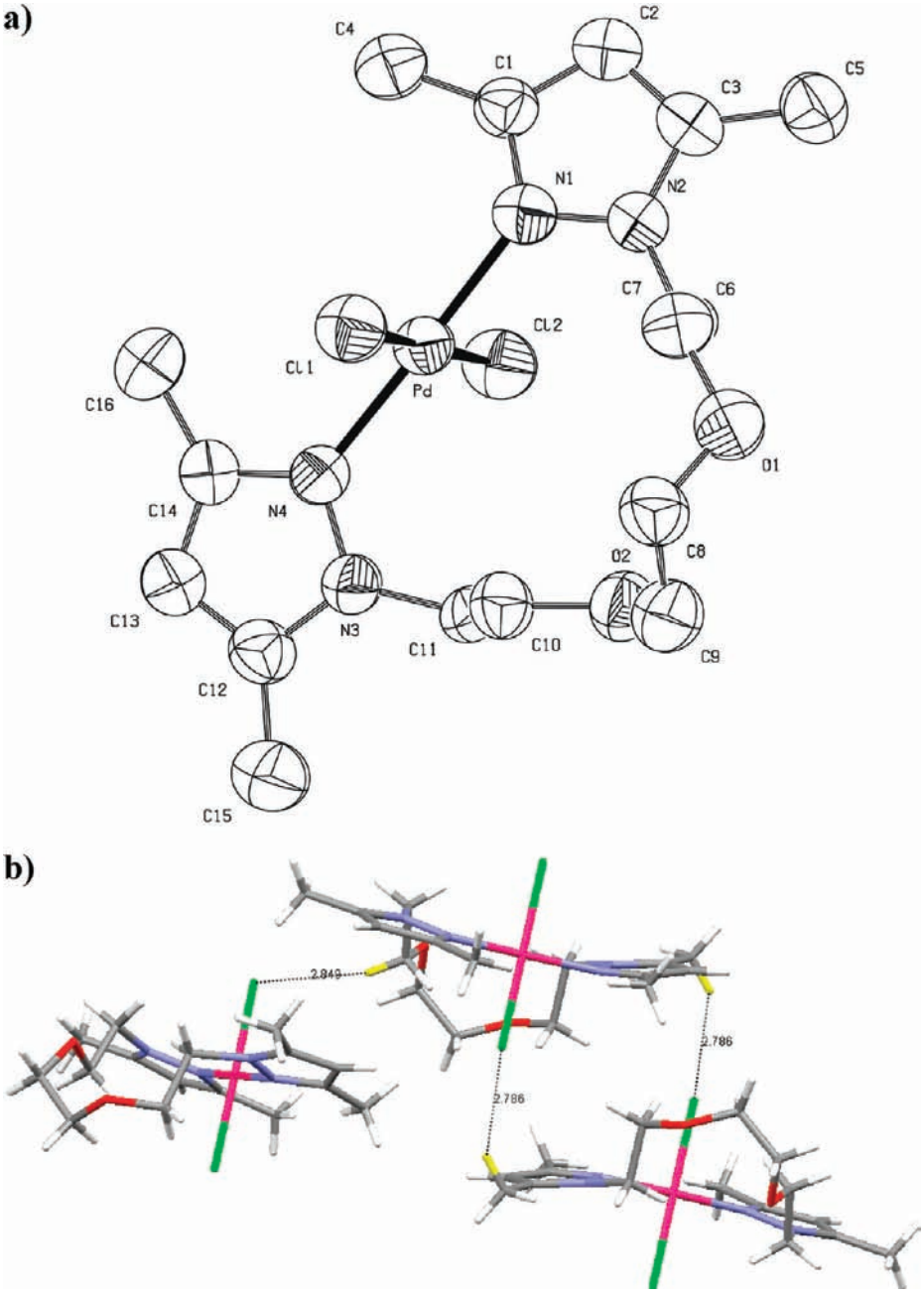

Figure 4. (a) ORTEP diagram of complex **4** showing an atom labeling scheme. 50% probability amplitude displacement ellipsoids are shown. Hydrogen atoms are omitted for clarity. See Table 2 for selected values of the bond lengths and bond angles. (b) View of some bonding interactions in the crystal structure.

anions, in particular, have been well-appreciated in recent times. Such interactions have been shown to be capable of playing a decisive role in the supramolecular structure of solids.[24] All the bonding parameters of these complexes are gathered in Table 6. The crystal structure of **1** consists of antiparallel chains of $[ZnCl_2(L)]$ units (Figure 2b) where the bonding interactions C−H···O (2.565 Å) form a 2D zigzag network. However, in the crystal structure of complex **2** ($M = Cd^{II}$) the oxygen atom does not play any role in this kind of interactions probably because of its participation in the coordination to the metallic center. In this case, the most important interactions are C−H···N (2.669 Å) and C−H···Cl (2.773 Å) (Figure 3b) which form an interconnected supramoleculars network. For complexes **4** ($M = Pd^{II}$) and **6** ($M = Pt^{II}$), the main bonding interactions are C−H···Cl−M (2.776−2.892 Å) (Figure 4b and 5b) which, as previously mentioned, are becoming a rapidly developing area of supramolecular chemistry. In complex **6**, the molecule of THF also participates with a C−H···O interaction (Figure 5b).

(24) (a) Aullón, G.; Bellamy, D.; Brammer, L.; Bruton, E. A.; Orpen, A. G. *Chem. Commun.* **1998**, *6*, 653–654. (b) Balamurugan, V.; Mukherjee, J.; Hundal, M. S.; Mukherjee, R. *Struct. Chem.* **2007**, *18*, 133–144. (c) Aakeröy, C. B.; Evans, T. A.; Seddon, K. R.; Pálinkó, I. *New J. Chem.* **1999**, *23*, 145–152. (d) Thallapally, P. K.; Nangia, A. *CrystEngComm* **2001**, *27*, 1–6. (e) Favero, L. B.; Giuliano, B. M.; Melandri, S.; Maris, A.; Ottaviani, P.; Velino, B.; Caminati, W. *J. Phys. Chem. A* **2005**, *109*, 7402–7404. (f) Calhorda, M. J. *Chem. Commun.* **2000**, *10*, 801–809.

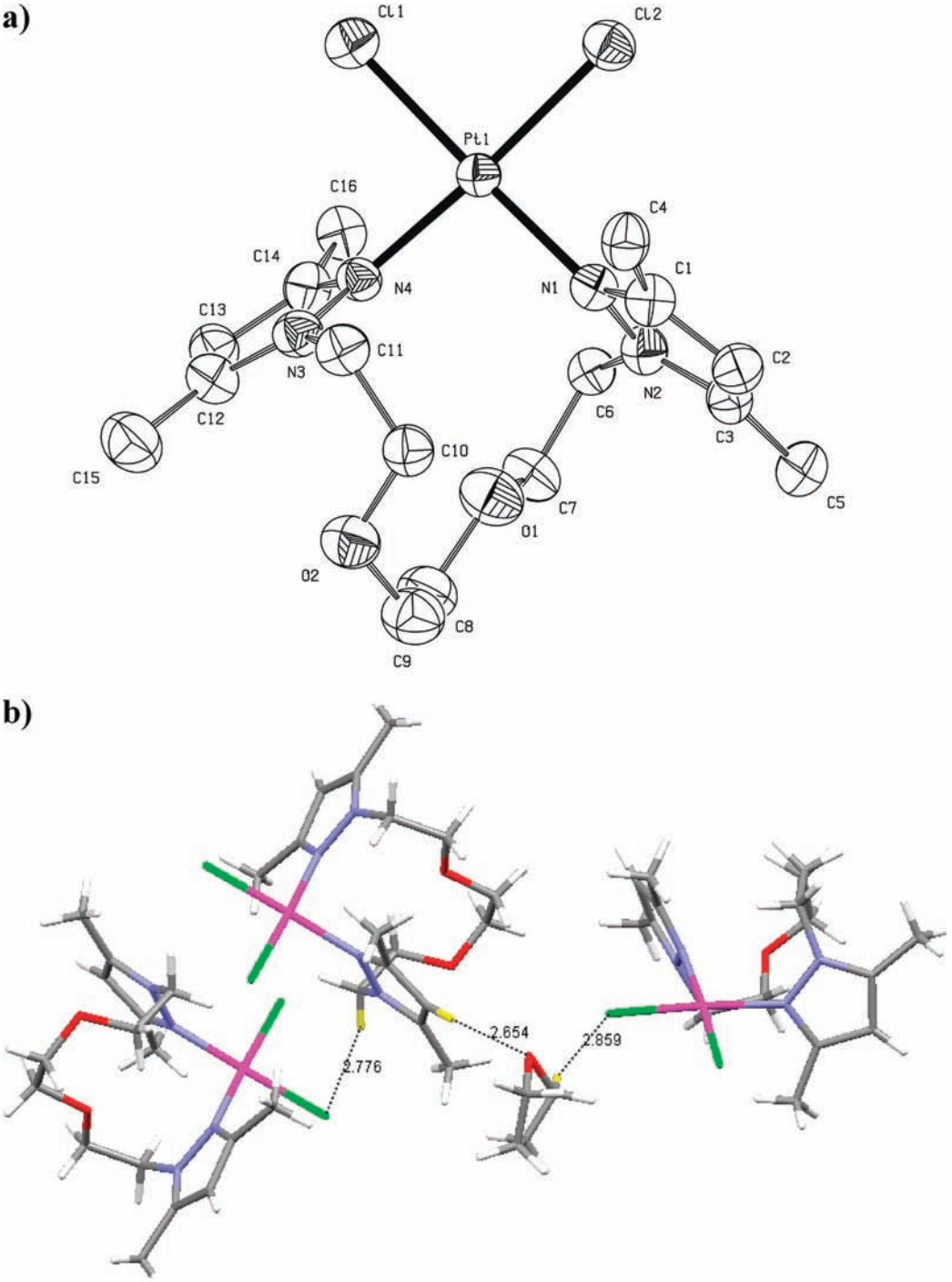

Figure 5. (a) ORTEP diagram of complex **6** showing an atom labeling scheme. 50% probability amplitude displacement ellipsoids are shown. Hydrogen atoms are omitted for clarity. See Table 2 for selected values of the bond lengths and bond angles. (b) View of some bonding interactions in the crystal structure.

Finally, in complex **7′**, apart from the hydrogen bondings mentioned above, there are other new interactions, C−H···Cl^- (2.641−2.820 Å) (Figure 6b). For all complexes the C−H···Cl intermolecular contacts have been categorized as intermediate (2.52−2.95 Å) (cf. sum of van der Waals radii for H and Cl = 2.95 Å).[24a]

NMR Spectra. At room temperature (RT), the ethylene protons of the OCH_2CH_2O chain for complexes $[MCl_2(L)]$ (M = Cd^{II} (**2**), Hg^{II} (**3**), Pd^{II} (**4**), and Pt^{II} (**6**)] appear as a singlet ($\delta(^1H)$ (ppm) = 3.48 (**2**); 3.44 (**3**); 3.92 (**4**), and 3.88 (**6**)) whereas the ethylene protons of the $N_{pz}CH_2CH_2O$ chain appear as two triplets ($\delta(^1H)$ (ppm) = 4.17, 3.76 (**2**); 4.09, 3.69 (**3**); 5.16, 4.20 (**4**), and 5.10, 4.16 (**6**)) with values of $^3J_{HH}$ (5.5−8.5 Hz). However, if we compare the ^1H NMR spectra of Zn^{II} (**1**) and Cd^{II} (**2**) complexes we can observe that, for complex **1** (Zn^{II}), the ethylene protons of OCH_2CH_2O and $N_{pz}CH_2CH_2O$ chains appear at lower fields and as broad bands at 3.73 ppm, and 4.57 ppm, 3.98 ppm, respectively (See Supporting Information). The presence of this kind of bands in the ^1H NMR spectra of Zn^{II} complex may be explained by the different coordination mode of **L** with Zn^{II} (κ^2 *NN*)

Table 4. Crystallographic data for **4**, **6**, and **7′**

	4 (Pd^{II})	**6** (Pt^{II})	**7′** (Ni^{II})
molecular formula	$C_{36}H_{62}Cl_4N_8O_5Pd_2$	$C_{20}H_{34}Cl_2N_4O_3Pt$	$C_{16}H_{30}Cl_2N_4O_4Ni$
formula weigh	1041.54	644.50	472.05
temperature (K)	293(2)	293(2)	293(2)
wavelength (Å)	0.71073	0.71073	0.71073
system, space group	monoclinic, $C2/c$	monoclinic, $P2_1/c$	monoclinic, Cc
unit cell dimensions			
a (Å)	30.931 (10)	11.259 (4)	16.654 (9)
b (Å)	11.018 (5)	14.594 (4)	9.433 (5)
c (Å)	16.001 (6)	14.691 (4)	15.762 (10)
α (deg)	90	90	90
β (deg)	120.20 (3)	91.96 (2)	120.76 (4)
γ (deg)	90	90	90
U (Å^3)	4713 (3)	2412.5 (13)	2128 (2)
Z	4	4	4
D_{calc} (g cm^{-3})	1.468	1.774	1.474
μ (mm^{-1})	1.036	6.066	1.191
F(000)	2136	1272	992
Crystal size (mm^3)	0.2 × 0.1 × 0.1	0.2 × 0.1 × 0.1	0.2 × 0.1 × 0.1
hkl ranges	$-46 \le h \le 46$	$-15 \le h \le 16$	$-22 \le h \le 24$
	$-15 \le k \le 16$	$-20 \le k \le 21$	$-13 \le k \le 12$
	$-23 \le l \le 23$	$-20 \le l \le 20$	$-21 \le l \le 21$
2θ range (deg)	2.70 to 32.33	2.64 to 32.25	2.59 to 32.38
reflections collected/unique/ [R_{int}]	23062/6639 [R(int) = 0.0572]	23600/7037 [R(int) = 0.0676]	10442/5410 [R(int) = 0.0385]
completeness to θ (θ = 25.00°)	97.2%	99.7%	95.4%
absorption correction	empirical	empirical	empirical
data/restrains/parameters	6639/33/283	7037/6/273	5410/9/260
goodness-of-fit on F^2	0.868	1.140	1.192
final R indices [$I > 2\sigma(I)$]	R1 = 0.0321, wR_2 = 0.0638	R1 = 0.0421, wR_2 = 0.1267	R1 = 0.0321, wR_2 = 0.0857
R indices (all data)	R1 = 0.0740, wR_2 = 0.0721	R1 = 0.0596, wR_2 = 0.1389	R1 = 0.0324, wR_2 = 0.0859
largest diff. peak and hole (e Å^{-3})	0.351 and −0.416	0.837 and −0.579	0.446 and −0.445

and Cd^{II} (κ^4 *NOON*) in solid state (Figure 2 and 3). In spite of that, we can not assert for complex **1** that it has the same polymeric structure as in solid state or that it has changed to a monomeric form.

Moreover, it has been possible to register $^{113}Cd\{^1H\}$ NMR (complex **2**), $^{199}Hg\{^1H\}$ NMR (complex **3**), and $^{195}Pt\{^1H\}$ NMR (complex **6**) spectra in D_2O (**2**, **3**) or $CDCl_3$ (**6**) at 298 K. These nuclei have spins 1/2 and offer several advantages including a larger chemical shift range, stronger heteronuclear coupling, and faster relaxation times. This kind of heteronuclear NMR spectroscopy is often applied on inorganic and organometallic compounds as a probe for structural and mechanistic studies of proteins containing Cd/Hg/Pt or those in which Zn is substituted by Cd/Hg at their active centers.[25] For complex **2**, the $^{113}Cd\{^1H\}$ NMR spectrum shows only one resonance at 50.1 ppm indicating the presence of a single hexacoordinated complex in solution (CN = 6; two N, two O, and two Cl atoms).[26] Furthermore, the information provided by this solution NMR experiment is corroborated in solid state by the X-ray diffraction of the crystal structure of **2**. In the same way, the Hg^{II} complex (**3**) shows one $^{199}Hg\{^1H\}$ NMR resonance at −1373 ppm suggesting a single hexacoordinated complex with similar coordination environment as in complex **2**.[27] Additionally, $^{195}Pt\{^1H\}$ NMR experiments for complex **6** reveal only one signal at −2208 ppm confirming the presence of a single complex in solution and illustrating how the platinum chemical shifts are sensitive to the average ligand environment. The chemical shifts for a PtN_2Cl_2 *core* are expected between −1998 and −2279 ppm.[28]

Interestingly, the ^1H NMR spectra of complexes **4** (Figure 7f) and **5** (Figure 7a) of Pd^{II} indicate the presence of two types of compounds: one species with a well-defined signal multiplicity (**4**) and another one with several broad resonances (**5**). Recently, we have demonstrated with a similar complex (**4A**) that the probable reason for this effect might be due to the presence of different stable conformers with significant population between 253 and 323 K.[6j] Theoretical calculations were carried out, and we obtained for the dimeric complex eight different conformers in a range of 5.8 kcal mol^{-1}. These conformers would only be interchangeable through high-energy barriers. Because of the higher flexibility of **L**, the dimeric complex **5** probably has a smaller number of conformers and/or has a lower energy barrier. The presence of monomeric and dimeric complexes of palladium in solution has been evidenced through diffusion NMR experiments in CD_3CN.

Diffusion NMR Studies of Complexes 4 and 5. These experiments are a powerful method to provide information about the relative size of the molecules in solution.[29]

(25) (a) Vig, K.; Megharaj, M.; Sethunathan, N.; Naidu, R. *Adv. Environ. Res.* **2003**, *8*, 121–135. (b) Sigel, A.; Sigel, H. *Metal Ions In Biological Systems*; Dekker: New York, 1997; Vol. *34*. (c) Ellis, P. D. *Science* **1983**, *221*, 1141–1146. (d) Utschig, L. M.; Wright, J. G.; Dieckmann, G.; Pecoraro, V.; O'Halloran, T. V. *Inorg. Chem.* **1995**, *34*, 2497–2498.

(26) (a) Reger, D. L.; Collins, J. E.; Myers, S. M.; Rheingold, A. L.; Liable-Sands, L. M. *Inorg. Chem.* **1996**, *35*, 4904–4909. (b) Summers, M. F. *Coord. Chem. Rev.* **1998**, *86*, 43–134.

(27) Helm, M. L.; Helton, G. P.; VanDerveer, D. G.; Grant, G. J. *Inorg. Chem.* **2005**, *44*, 5696–5705.

(28) (a) Trávnicek, Z.; Malon, M.; Zatloukal, M.; Dolezal, K.; Strnad, K.; Marek, J. *J. Inorg. Biochem.* **2003**, *94*, 307–316. (b) Tsiveriotis, P.; Hadjiliadis, N.; Slauropoules, G. *Inorg. Chim. Acta* **1997**, *261*, 83–92. (c) Tessier, C.; Rochon, F. D. *Inorg. Chim. Acta* **1999**, *295*, 25–38. (d) Pregosin, P. S. *Coord. Chem. Rev.* **1982**, *33*, 247–291.

(29) Valentini, M.; Rüegger, H.; Pregosin, P. S. *Organometallics* **2000**, *19*, 2551–2555.

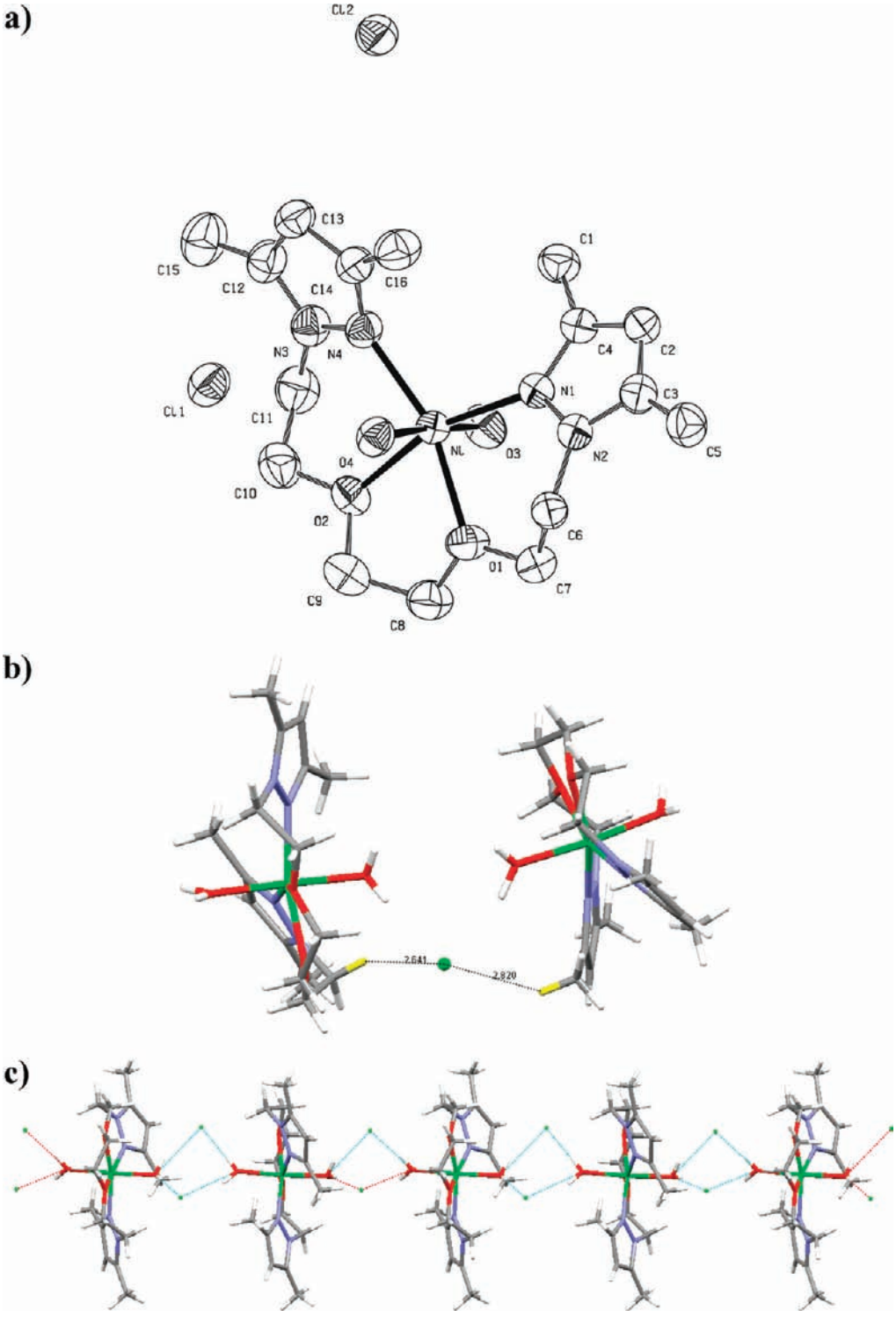

Figure 6. (a) ORTEP diagram of complex **7′** showing an atom labeling scheme. 50% probability amplitude displacement ellipsoids are shown. Hydrogen atoms are omitted for clarity. See Table 2 for selected values of the bond lengths and bond angles. (b) View of some bonding interactions in the crystal structure. (c) View of hydrogen bonding in the crystal structure of $[Ni(H_2O)_2(L)]Cl_2$ (**7′**) forming an infinite chain.

Measurement of the diffusion coefficients (D) was made from DOSY spectra of a mixture of compounds **4** and **5** at 298 K in a CD_3CN solution. The monomer **4** (MW = 483.7 g mol^{-1}) presents a D value of (12.3 ± 0.08) × 10^{-10} m^2 s^{-1} that is equivalent to a hydrodynamic radius (R_H) of 5.87 ± 0.60 Å. In contrast, the D value of the dimer **5** (MW = 967.5 g mol^{-1}) was determined as (9.51± 0.08) × 10^{-10} m^2 s^{-1}, with R_H of 7.57 ± 0.60 Å. The hydrodynamic radius of the monomeric complex **4** is in qualitative agreement with the crystal structural radius (R_E; 5.83 Å). Interestingly, comparing the diffusion coefficients of **4** (12.3) and **4A** (11.2) it is noted that **L** provokes an increase in D and, consequently, a decrease of the hydrodynamic radius (5.87 (**4**); 6.43 (**4A**)). Assuming that both dimer and monomer derivatives present similar shapes, the predicted ratio between their radii

Table 5. Distances (Å) and Angles (deg) Related to Hydrogen Bonding in Complex **7′**

	D−H	D···A	A···H	D−H···A	symmetry code
O (3)−H (1O)···Cl (1)	0.80 (4)	3.071 (3)	2.33 (4)	155 (4)	
O (3)−H (2O)···Cl (2)	0.81 (4)	3.071 (3)	2.28 (4)	167 (4)	$x, -1 + y, z$
O (4)−H (3O)···Cl (1)	0.80 (3)	3.097 (3)	2.33 (5)	163 (3)	$x, -y, -1/2 + z$
O (4)−H (4O)···Cl (2)	0.92 (5)	3.196 (3)	2.32 (5)	160 (4)	$x, 1 - y, -1/2 + z$

Table 6. Bonding Interactions C−H···X (X = O, N or Cl/Cl^-) Parameters for Complexes **1**, **2**, **4**, **6**, and **7′**

complex	D−H···A	H···A (Å)	D···A (Å)	D−H···A (deg)
1 (Zn^{II})	C (5)−H (5A)···O (1)	2.565	3.340	137.96
2 (Cd^{II})	C (5)−H (5B)···N (2)	2.669	3.588	160.75
	C (6)−H (6A)···Cl (1)	2.880	3.604	132.11
	C (8)−H (8A)···Cl (1)	2.773	3.718	164.91
4 (Pd^{II})	C (5)−H (5B)···Cl (1)	2.786	3.613	144.88
	C (10)−H (10B)···Cl (2)	2.849	3.783	161.53
6 (Pt^{II})	C (6)−H (6B)···Cl (1)	2.892	3.852	170.54
	C (11)−H (11A)···Cl (2)	2.776	3.695	158.33
	C (13)−H (13)···O (3)	2.654	3.582	174.94
	C (20)−H (20B)···Cl (1)	2.859	3.744	153.07
7' (Ni^{II})	C (1)−H (1B)···Cl (2)	2.820	3.596	138.62
	C (6)−H (6A)···Cl (2)	2.641	3.484	145.57
	C (6)−H (6B)···Cl (1)	2.785	3.572	138.68

should be about 1.26. This value is in close analogy to the ratio obtained experimentally for **4**/**5** (1.29). As we have shown, monomeric and dimeric palladium(II) complexes coexist in a CD_3CN solution, and no interconversion between them could be observed. They have been fully characterized by 1D and 2D NMR spectroscopy.

It is really interesting to emphasize the solvent effect in the reaction between **L** ligand and Pd^{II}. As we have described above, monomeric complex (**4**) was obtained when the solvent of the reaction is acetonitrile whereas dimeric complex (**5**) was obtained as long as the solvent is THF or CH_2Cl_2. A similar effect has been published recently by our group with modified ligands of **L** introducing a phenyl group in the chain in different relative positions (ortho, meta, and para).[6j] However, the reaction of these ligands bis[4-(3,5-dimethyl-1*H*-pyrazol-1-yl)-2-oxabutyl]benzene with Pd^{II} in CH_2Cl_2 yields a mixture of monomeric/dimeric compounds. Unfortunately, we can not justify with total accuracy the exact reason for this behavior. However, this effect made by the solvent in synthesis of metallo-macrocycles, it is also observed in other research groups, for example, by Fujita et al. (with DMSO and CH_3CN).[30]

In addition to that, another aspect to consider is the role of the heteroatom located in the chain of the hybrid ligand. In our group other studies have been conducted with similar ligands containing sulfur in stead of oxygen. For instance, with the analogous ligand of **L**, 1,8-bis(3,5-dimethyl-1*H*-pyrazol-1-yl)-3,6-dithiaoctane; the results indicate that this kind of ligands do not show the same behavior toward Pd^{II} (effect of the solvent) as the ones presented on this paper with the same conditions. So, with *N*-pyrazole and *S*-thioether ligands, Pd^{II} dimeric complexes have not been observed.[19]

Conversion of Binuclear Complex 5 to Mononuclear Complex 4. As in our recently published work with *N, O*-hybrid pyrazole ligand (**LA**),[6j] we have also observed that the dimeric complex (**5**) is converted into the analogous monomeric complex (**4**) (Figure 7). The conversion was studied in CH_3CN at 333 K to obtain the thermodynamically favored product, complex **4** (168 h). In comparison with **4A** (24 h), we have obtained longer conversion time probably because of the higher flexibility of **L**. Moreover, theoretical calculations showed that the dimerization of monomer **4A** is energetically favorable ($\Delta E = -4.9$ kcal mol^{-1}), but entropy makes the process thermodynamically unfavorable at 25 °C ($\Delta G° = 7.2$ kcal mol^{-1}). Similar conversions have been observed in other systems and, as expected, dimerization of the monomeric complex (**4**) in THF has not been observed.[31]

Conclusion

A series of Zn^{II} (**1**), Cd^{II} (**2**), Hg^{II} (**3**), Pd^{II} (**4** and **5**), Pt^{II} (**6**), and Ni^{II} (**7**) complexes with the new hybrid pyrazole ligand, 1,8-bis(3,5-dimethyl-1*H*-pyrazol-1-yl)-3,6-dioxaoctane, (**L**) have been successfully synthesized and characterized. Heteronuclear magnetic resonance ($^{113}Cd\{^1H\}$, $^{199}Hg\{^1H\}$, and $^{195}Pt\{^1H\}$) spectroscopy was useful to find out the geometry and the coordination environment of the metallic center of complexes **2**, **3**, and **6**. Moreover, monomeric and dimeric compounds of Pd^{II} (**4** and **5**) have been characterized in solution through diffusion NMR studies. It has been observed that the dimeric complex is converted into the corresponding monomer in an acetonitrile reflux, thus indicating that the latter is thermodynamically more stable than the dimer.

The versatility of **L** is demonstrated because of the denticity of the ligand is found to vary from *NN*-bidentate (chelate or bridge) to *NOON*-tetradentate (equatorial or axial) as confirmed in the solid state by single-crystal X-ray diffraction studies. Moreover, the ligand is also found to accommodate a range of metal coordination geometries (tetrahedral,

(30) Suzuki, K.; Kawano, M.; Fujita, M. *Angew. Chem., Int. Ed.* **2007**, *46*, 2819–2822.

(31) (a) Hollyday, B. J.; Mirkin, C. A. *Angew. Chem., Int. Ed.* **2001**, *40*, 2022–2043. (b) Farrell, J. R.; Eisenberg, A. H.; Mirkin, C. A.; Guzei, I. A.; Liable-Sands, L. M.; Incarvito, C. D.; Rheingold, A. L.; Stern, C. L. *Organometallics* **1999**, *18*, 4856–4868.

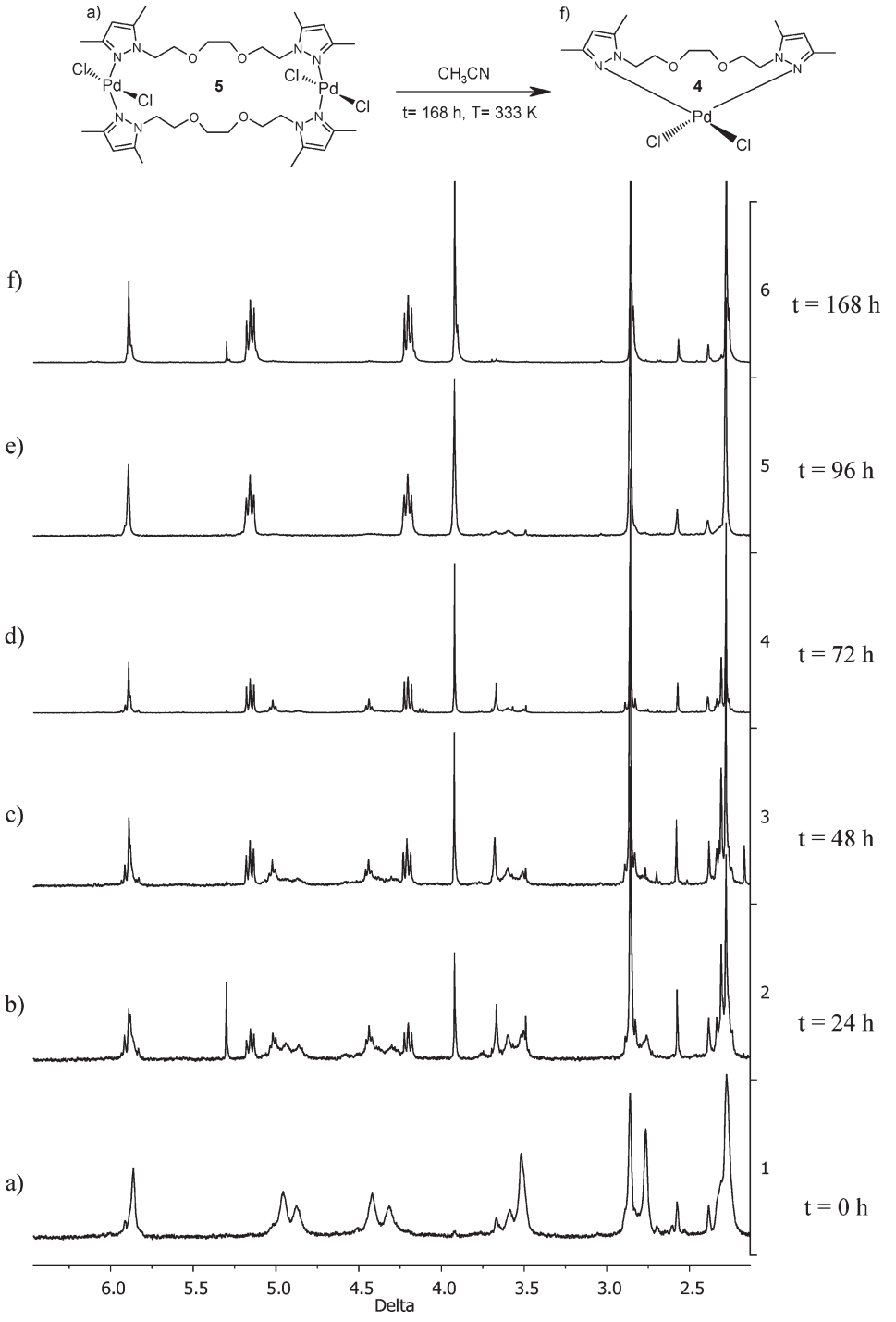

Figure 7. Monitoring by ^{1}H NMR, of conversion of dimeric complex **5** to the corresponding monomeric complex **4** in CH_3CN at 333 K during 168 h (a−f).

cis/*trans*-square planar, or octahedral) and nuclearity (monomer or dimer), as a consequence of the coordination requirement of the metals, the reaction conditions, and the variety of the donor atoms. Such characteristics of **L** have considerable merits for their use in catalysis. Current work is focused on exploring the potential of some of these complexes as catalysts for the Heck reaction.

Experimental Section

General Procedures. Unless otherwise noted, all reactions and manipulations were carried out under an atmosphere of dry nitrogen using vacuum line and standard Schlenk techniques. All solvents were dried and distilled according to standard procedures and stored under nitrogen.[32] Samples of $[PdCl_2(CH_3CN)_2]$ were prepared as described in the literature.[10]

Instrumentation. Melting points were measured on an Electrothermal 1A8104 melting point apparatus. Elemental analyses (C, H, and N) were carried out by the staff of Chemical Analyses Service of the Universitat Autònoma de Barcelona on a Eurovector 3011 instrument. Conductivity measurements were performed at RT in 10^{-3} M methanol or acetone solutions, employing a CyberScan CON 500 (Euthech instrument) conductimeter.

(32) Armarego, W. L. F.; Perrin, D. *Purification of Laboratory Chemicals*; Butterworth-Heinemann: Oxford, 1996.

Infrared spectra were run on a Perkin-Elmer FT spectrophotometer, series 2000 cm^{-1} as KBr pellets or polyethylene films in the range 4000−150 cm^{-1}. Electronic spectra were run on a Kontron-Uvikon 860 in methanol between 750 and 350 nm. ^1H NMR, ^{13}C $\{^1H\}$ NMR, HSQC, COSY, and NOESY spectra were recorded on a Bruker AVANCE 250 MHz NMR spectrometer in $CDCl_3$ solutions at RT. 1D $^{195}Pt\{^1H\}$, $^{113}Cd\{^1H\}$, and $^{199}Hg\{^1H\}$ NMR spectra were recorded on a DPX-360 Bruker spectrometer equipped with a 5 mm broadband probe. All spectra were recorded at 298 K in $CDCl_3$ (^{195}Pt) or D_2O (^{113}Cd and ^{199}Hg), using a recycle time of 0.01 s (^{195}Pt) or 1 s (^{113}Cd and ^{199}Hg). Spectra were processed with a line broadening of 1 Hz prior to Fourier Transformation and externally referenced to aqueous solutions of $[PtCl_6]^{2-}$, 0.1 M $Cd(ClO_4)_2$ and 0.1 M of $Hg(ClO_4)_2$ in D_2O.[27] NMR diffusion experiments were carried out at 298 K in CD_3CN on a 500 MHz AVANCE spectrometer equipped with a 5 mm TCI cryoprobe. Self-diffusion experiments were performed using the compensated BPLED pulse sequence[33] to avoid unwanted convection effects, using a diffusion time of 150 ms and a LED delay of 5 ms. For each experiment, sine-shaped pulsed-field gradients with a duration of 1.5 ms followed by a recovery delay of 100 μs were incremented from 2% to 95% of the maximum strength in 16 equally spaced steps. Diffusion coefficients were obtained by measuring the slope in the following linear relationship: $\ln(A_g/A_o) = -\gamma^2 g^2 \delta^2 (4\Delta - \delta)D$; where A_g and A_o are the signal intensities in the presence and absence of pulsed field gradient (PFG), respectively, γ is the gyromagnetic ratio (rad $s\ g^{-1}$), g is the strength of the diffusion gradients (G cm^{-1}), D is the diffusion coefficient of the observed spins ($m^2\ s^{-1}$), δ is the length of the diffusion gradient (s), and Δ is the time separation between the leading edges of the two diffusion pulsed gradients (s). All chemical shifts values (δ) are given in ppm. Electrospray mass spectra were obtained with an Esquire 3000 ion trap mass spectrometer from Bruker Daltonics.

Synthesis of Ligand L. A solution of 2.90 g (0.030 mol) of 3,5-dimethylpyrazole in 50 mL of THF was slowly added to a suspension of 0.80 g (0.033 mol) of NaH in 10 mL of THF. The solution was stirred at 60 °C for 2 h. To the resulting solution was added dropwise with stirring a solution of 2.82 g (0.015 mol) of 1,2-bis(2-chloroethoxy)ethane in 10 mL of THF. The resulting mixture was allowed to stir for 12 h at 60 °C. After cooling to RT, 10 mL of water was added dropwise to destroy excess NaH. The solvents were then evaporated under reduced pressure. The residue was taken up in water (40 mL) and extracted with chloroform (3 × 50 mL). The chloroform layers were dried with anhydrous $MgSO_4$ and evaporated to give a white solid.

L. Yield: 86% (3.97 g). mp 57.3−58.2 °C. $C_{16}H_{26}N_4O_2$: Anal. Calcd for $C_{16}H_{26}N_4O_2$: C, 62.72; H, 8.55; N, 18.29. Found: C, 62.92; H, 8.28; N, 18.14. MS m/z (%) = 329.1 (100%) $[M+Na]^+$. IR (KBr, cm^{-1}): 3121 [ν(C−H)$_{ar}$], 2960, 2880 [ν(C−H)$_{al}$], 1551 [(ν(C=C), ν(C=N))$_{ar}$], 1430 [(δ(C=C), δ(C=N))$_{ar}$], 1087 [ν(C−O−C)], 781, 769 [δ(C−H)$_{oop}$]. ^1H NMR ($CDCl_3$ solution, 250 MHz): δ 5.73 (s, 2H, CH(pz)), 4.08 (t, 4H, ^3J = 5.7 Hz, $N_{pz}CH_2CH_2O$), 3.73 (t, 4H, ^3J = 5.7 Hz, $N_{pz}CH_2CH_2O$), 3.44 (s, 4H, OCH_2CH_2O), 2.21 (s, 6H, CH_3(pz)), 2.19 (s, 6H, CH_3-(pz)) ppm. $^{13}C\{^1H\}$ NMR ($CDCl_3$ solution, 63 MHz): δ 147.6 (pz-C), 139.9 (pz-C), 104.8 (CH(pz)), 70.7 (OCH_2CH_2O), 70.4 ($N_{pz}CH_2CH_2O$), 48.5 ($N_{pz}CH_2CH_2O$), 13.5 (CH_3(pz)), 11.1 (CH_3(pz)) ppm.

Synthesis of Complexes $[MCl_2(L)]$ (M = Zn^{II} (1), Cd^{II} (2), Hg^{II} (3)). An absolute ethanol solution (10 mL) of the **L** ligand (0.225 g, 0.73 mmol) was added to an absolute ethanol solution (20 mL) of $ZnCl_2$ (0.100 g, 0.73 mmol) for **1**, $CdCl_2$ (0.134 g, 0.73 mmol) for **2**, or $HgCl_2$ (0.199 g, 0.73 mmol) for **3**, and 4 mL of triethyl orthoformate (for dehydration purposes). The resulting solution was allowed to stir for 2 h at RT. The solvent was removed in vacuo to yield a white solid in all cases, which was filtered off, washed twice with 5 mL of diethyl ether and dried in vacuum.

1. Yield: 78% (0.254 g). Anal. Calcd for $C_{16}H_{26}Cl_2N_4O_2Zn$: C, 43.41; H, 5.92; N, 12.66. Found: C, 43.40; H, 5.85; N, 12.62. Conductivity (S $cm^2\ mol^{-1}$, 1.12 10^{-3} M in MeOH): 37.2. MS m/z (%) = 407.0 (100%) $[M-Cl]^+$. IR (KBr, cm^{-1}): 3125 [ν(C−H)$_{ar}$], 2966, 2875 [ν(C−H)$_{al}$], 1553 [(ν(C=C), ν(C=N))$_{ar}$], 1423 [(δ(C=C), δ(C=N))$_{ar}$], 1115 [ν(C−O−C)], 827 [δ(C−H)$_{oop}$]. (Polyethylene, cm^{-1}): 485 [ν(Zn−N)]. ^1H NMR ($CDCl_3$ solution, 250 MHz): δ 5.95 (s, 2H, CH(pz)), 4.57 (m, 4H, $N_{pz}CH_2CH_2O$), 3.98 (m, 4H, $N_{pz}CH_2CH_2O$), 3.73 (m, 4H, OCH_2CH_2O), 2.41 (s, 6H, CH_3(pz)), 2.30 (s, 6H, CH_3-(pz)) ppm. $^{13}C\{^1H\}$ NMR ($CDCl_3$ solution, 63 MHz): δ 153.6 (pz-C), 141.1 (pz-C), 107.8 (CH(pz)), 71.1 (OCH_2CH_2O), 70.3 ($N_{pz}CH_2CH_2O$), 48.3 ($N_{pz}CH_2CH_2O$), 13.6 (CH_3(pz)), 11.6 (CH_3(pz)) ppm.

2. Yield: 89% (0.319 g). Anal. Calcd for $C_{16}H_{26}Cl_2N_4O_2Cd$: C, 39.24; H, 5.35; N, 11.44. Found: C, 39.17; H, 5.55; N, 11.31. Conductivity (S $cm^2\ mol^{-1}$, 1.15 10^{-3} M in MeOH): 27.8. MS m/z (%) = 454.3 (100%) $[M-Cl]^+$. IR (KBr, cm^{-1}): 3125 [ν(C−H)$_{ar}$], 2971, 2878 [ν(C−H)$_{al}$], 1554 [(ν(C=C), ν(C=N))$_{ar}$], 1468 [(δ(C=C), δ(C=N))$_{ar}$], 1097 [ν(C−O−C)], 825 [δ(C−H)$_{oop}$]. (Polyethylene, cm^{-1}): 492 [ν(Cd−N)]. ^1H NMR ($CDCl_3$ solution, 250 MHz): δ 5.78 (s, 2H, CH(pz)), 4.17 (t, 4H, ^3J = 5.6 Hz, $N_{pz}CH_2CH_2O$), 3.76 (t, 4H, ^3J = 5.6 Hz, $N_{pz}CH_2CH_2O$), 3.48 (s, 4H, OCH_2CH_2O), 2.22 (s, 12H, CH_3-(pz)) ppm. $^{13}C\{^1H\}$ NMR ($CDCl_3$ solution, 63 MHz): δ 149.1 (pz-C), 142.3 (pz-C), 105.1 (CH(pz)), 69.8 (OCH_2CH_2O), 69.4 ($N_{pz}CH_2CH_2O$), 47.7 ($N_{pz}CH_2CH_2O$), 12.2 (CH_3(pz)), 10.1 (CH_3(pz)) ppm. $^{113}Cd\{^1H\}$ NMR (D_2O solution, 88.12 MHz): δ 50.1 ppm.

3. Yield: 93% (0.394 g). Anal. Calcd for $C_{16}H_{26}Cl_2N_4O_2Hg$: C, 33.25; H, 4.53; N, 9.69. Found: C, 33.13; H, 4.58; N, 9.45. Conductivity (S $cm^2\ mol^{-1}$, 1.17 10^{-3} M in MeOH): 21.4. MS m/z (%) = 543.2 (100%) $[M-Cl]^+$. IR (KBr, cm^{-1}): 3129 [ν(C−H)$_{ar}$], 2915, 2863 [ν(C−H)$_{al}$], 1550 [(ν(C=C), ν(C=N))$_{ar}$], 1468 [(δ(C=C), δ(C=N))$_{ar}$], 1109 [ν(C−O−C)], 805 [δ(C−H)$_{oop}$]. (Polyethylene, cm^{-1}): 487 [ν(Hg−N)]. ^1H NMR ($CDCl_3$ solution, 250 MHz): δ 5.92 (s, 2H, CH(pz)), 4.43 (t, 4H, ^3J = 5.8 Hz, $N_{pz}CH_2CH_2O$), 3.85 (t, 4H, ^3J = 5.8 Hz, $N_{pz}CH_2CH_2O$), 3.68 (s, 4H, OCH_2CH_2O), 2.34 (s, 6H, CH_3-(pz)), 2.29s, 6H, CH_3(pz)) ppm. $^{13}C\{^1H\}$ NMR ($CDCl_3$ solution, 63 MHz): δ 148.9 (pz-C), 142.4 (pz-C), 106.2 (CH(pz)), 71.7 (OCH_2CH_2O), 71.3 ($N_{pz}CH_2CH_2O$), 46.3 ($N_{pz}CH_2CH_2O$), 13.5 (CH_3(pz)), 11.2 (CH_3(pz)) ppm. $^{199}Hg\{^1H\}$ NMR (D_2O solution, 64.43 MHz): δ −1373 ppm.

Synthesis of Complexes $[PdCl_2(L)]$ (4) and $[PdCl_2(L)]_2$ (5). A CH_3CN solution (20 mL) for **4** or a THF solution (20 mL) for **5** of $[PdCl_2(CH_3CN)_2]$ (70 mg, 0.270 mmol) was added to a CH_3CN solution (5 mL) (**4**) or to a THF solution (5 mL) (**5**) of the **L** ligand (83 mg, 0.270 mmol), and the resulting solution was allowed to stir for 36 h at 60 °C (**4**) or 12 h at RT (**5**). The solvent was removed in vacuo to yield a yellow solid, which was filtered off, washed with 10 mL of diethyl ether and dried in vacuum.

4. Yield: 75% (0.098 g). Anal. Calcd for $C_{16}H_{26}Cl_2N_4O_2Pd$: C, 39.73; H, 5.42; N, 11.58. Found: C, 39.72; H, 5.31; N, 11.29. Conductivity (S $cm^2\ mol^{-1}$, 1.17 10^{-3} M in MeOH): 46.9. MS m/z (%) = 447.0 (100%) $[M-Cl]^+$, 507.0 (18%) $[M+Na]^+$. IR (KBr, cm^{-1}): 3129 [ν(C−H)$_{ar}$], 2954, 2855 [ν(C−H)$_{al}$], 1556 [(ν(C=C), ν(C=N))$_{ar}$], 1423 [(δ(C=C), δ(C=N))$_{ar}$], 1117 [ν(C−O−C)], 794 [δ(C−H)$_{oop}$]. (Polyethylene, cm^{-1}): 491 [ν(Pd−N)], 347 [ν(Pd−Cl)]. ^1H NMR ($CDCl_3$ solution, 250 MHz): δ 5.89 (s, 2H, CH(pz)), 5.16 (t, 4H, ^3J = 8.1 Hz, $N_{pz}CH_2CH_2O$), 4.20 (t, 4H, ^3J = 8.1 Hz, $N_{pz}CH_2CH_2O$), 3.92 (s, 4H, OCH_2CH_2O), 2.86 (s, 6H, CH_3(pz)), 2.28 (s, 6H, CH_3-(pz)) ppm. $^{13}C\{^1H\}$ NMR ($CDCl_3$ solution, 63 MHz): δ 150.6

(33) Jerschow, A.; Muller, N. *J. Magn. Reson.* **1997**, *125*, 372–375.

(pz-*C*), 143.3 (pz-*C*), 108.0 (*C*H(pz)), 70.8 (O*C*H$_2$*C*H$_2$O), 68.2 (N$_{pz}$CH$_2$*C*H$_2$O), 49.3 (N$_{pz}$*C*H$_2$CH$_2$O), 15.1 (*C*H$_3$(pz)), 11.9 (*C*H$_3$(pz)) ppm.

5. Yield: 79% (0.104 g). Anal. Calcd for $C_{32}H_{52}Cl_4N_8O_4Pd_2$: C, 39.73; H, 5.42; N, 11.58. Found: C, 39.59; H, 5.57; N, 11.45. Conductivity (S cm^2 mol^{-1}, 1.04 10^{-3} M in MeOH): 30.4. MS *m*/*z* (%) = 988.9 (62%) [M+Na]$^+$, 933.0 (100%) [M−Cl]$^+$. IR (KBr, cm^{-1}): 3130 [ν(C−H)$_{ar}$], 2919, 2868 [ν(C−H)$_{al}$], 1556 [(ν(C=C), ν(C=N))$_{ar}$], 1423 [(δ(C=C), δ(C=N))$_{ar}$], 1111 [ν(C−O−C)], 800 [δ(C−H)$_{oop}$]. (Polyethylene, cm^{-1}): 496 [ν(Pd−N)], 352 [ν(Pd−Cl)]. ^{1}H NMR (CDCl$_3$ solution, 250 MHz): δ 5.87 (s, 2H, C*H*(pz)), 4.96 (m, 4H, N$_{pz}$*CH*$_2$CH$_2$O), 4.42 (m, 4H, N$_{pz}$CH$_2$C*H*$_2$O), 3.52 (m, 4H, OC*H*$_2$C*H*$_2$O), 2.86 (m, 6H, C*H*$_3$(pz)), 2.25 (m, 6H, C*H*$_3$(pz)) ppm. ^{13}C{^{1}H} NMR (CDCl$_3$ solution, 63 MHz): δ 150.5 (pz-*C*), 145.0 (pz-*C*), 107.7 (*C*H(pz)), 70.9 (O*C*H$_2$*C*H$_2$O), 69.6 (N$_{pz}$CH$_2$*C*H$_2$O), 50.2 (N$_{pz}$*C*H$_2$CH$_2$O), 15.2 (*C*H$_3$(pz)), 12.2 (*C*H$_3$(pz)) ppm.

Synthesis of Complex [PtCl$_2$(L)] (6). To a solution of K_2PtCl_4 (70 mg, 0.170 mmol) in 10 mL of distilled water was added 103 mg (0.170 mmol) of the **L** ligand suspended in 10 mL of the same solvent. The resulting solution was refluxed for 2 h. The aqueous phase was extracted twice with 10 mL of CH_2Cl_2. Water was removed under reduced pressure yielding a yellow solid.

6. Yield: 21% (0.020 g). Anal. Calcd for $C_{16}H_{26}Cl_2N_4O_2Pt$: C, 33.57; H, 4.58; N, 9.79. Found: C, 33.45; H, 4.69; N, 10.01. Conductivity (S cm^2 mol^{-1}, 1.04 10^{-3} M in MeOH): 35.3. MS *m*/*z* (%) = 595.1 (100%) [M+Na]$^+$. IR (KBr, cm^{-1}): 3128 [ν(C−H)$_{ar}$], 2920, 2878 [ν(C−H)$_{al}$], 1556 [(ν(C=C), ν(C=N))$_{ar}$], 1422 [(δ(C=C), δ(C=N))$_{ar}$], 1114 [ν(C−O−C)], 798 [δ(C−H)$_{oop}$]. (Polyethylene, cm^{-1}): 512 [ν(Pt−N)], 340, 328 [ν(Pt−Cl)]. ^{1}H NMR (CDCl$_3$ solution, 250 MHz): δ 5.90 (s, 2H, C*H*(pz)), 5.10 (t, 4H, ^3J = 8.5 Hz, N$_{pz}$*CH*$_2$CH$_2$O), 4.16 (t, 4H, ^3J = 8.5 Hz, N$_{pz}$CH$_2$C*H*$_2$O), 3.88 (s, 4H, OC*H*$_2$C*H*$_2$O), 2.79 (s, 6H, C*H*$_3$(pz)), 2.35 (s, 6H, C*H*$_3$(pz)) ppm. ^{13}C{^{1}H} NMR (CDCl$_3$ solution, 63 MHz): δ 150.1 (pz-*C*), 144.2 (pz-*C*), 107.3 (*C*H(pz)), 70.8 (O*C*H$_2$*C*H$_2$O), 69.4 (N$_{pz}$CH$_2$*C*H$_2$O), 48.9 (N$_{pz}$*C*H$_2$CH$_2$O), 15.2 (*C*H$_3$(pz)), 12.9 (*C*H$_3$(pz)) ppm. ^{195}Pt-{^{1}H} NMR (CDCl$_3$ solution, 77.42 MHz): δ −2208 ppm.

Synthesis of Complex [NiCl$_2$(L)] (7). An absolute ethanol solution (10 mL) of the **L** ligand (0.277 g, 0.90 mmol) was added to an absolute ethanol solution (20 mL) of $NiCl_2 \cdot 6H_2O$ (0.117 g, 0.90 mmol), and 4 mL of triethyl orthoformate (for dehydration purposes). The resulting solution was allowed to stir for 24 h at RT. The solvent was removed to yield a green solid, which was filtered off, washed twice with 5 mL of diethyl ether and dried in vacuum.

7. Yield: 75% (0.296 g). Anal. Calcd for $C_{16}H_{26}Cl_2N_4O_2Ni$: C, 44.08; H, 6.01; N, 12.85. Found: C, 44.17; H, 5.89; N, 12.93. Conductivity (S cm^2 mol^{-1}, 1.08 10^{-3} M in MeOH): 187.0; (1.14 10^{-3} M in acetone): 29.5. MS *m*/*z* (%) = 399.1 (100%) [M−Cl]$^+$. IR (KBr, cm^{-1}): 3128 [ν(C−H)$_{ar}$], 2932, 2891 [ν(C−H)$_{al}$], 1554 [(ν(C=C), ν(C=N))$_{ar}$], 1465 [(δ(C=C), δ(C=N))$_{ar}$], 1121 [ν(C−O−C)], 783 [δ(C−H)$_{oop}$]. (Polyethylene, cm^{-1}): 478 [ν(Ni−N)]. UV−vis (1.22 10^{-3} M in MeOH), λ(ε): 677(12), 581(17) nm; (1.14 10^{-3} M in acetone), λ(ε): 681(13), 595(21) nm.

X-ray Crystal Structure Analyses of Complexes 1, 2, 4, 6, and 7′. Suitable crystals for X-ray diffraction were obtained through crystallization from a diethyl ether/dichloromethane (1:1) mixture (compounds **1**, **2**, and **4**) or from a THF/dichloromethane (1:1) mixture (compounds **6** and **7′**).

A prismatic crystal was selected and mounted on a MAR345 diffractometer with an image plate detector. Unit-cell parameters were determined from 904 reflections for **1**, 825 reflections for **2**, 163 reflections for **4**, 426 reflections for **6**, and 403 reflections for **7′**, (3° < θ < 31°) and refined by least-squares method.

Intensities were collected with graphite monochromatized Mo Kα radiation. For **1**, 24866 reflections were measured in the range 2.73° ≤ θ ≤ 32.51°, of which 3557 were non-equivalent by symmetry (R_{int}(on *I*) = 0.035). A total of 1477 reflections were assumed as observed applying the condition $I \geq 2\sigma(I)$. For **2**, 14224 reflections were measured in the range 2.87° ≤ θ ≤ 30.23°, of which 2204 were non-equivalent by symmetry (R_{int}(on *I*) = 0.039). A total of 2149 reflections were assumed as observed applying the condition $I \geq 2\sigma(I)$. For **4**, 23062 reflections were measured in the range 2.70° ≤ θ ≤ 32.33°, of which 6639 were non-equivalent by symmetry (R_{int}(on *I*) = 0.057). A total of 4086 reflections were assumed as observed applying the condition $I \geq 2\sigma(I)$. For **6**, 23600 reflections were measured in the range 2.64° ≤ θ ≤ 32.25°, of which 7037 were non-equivalent by symmetry (R_{int}(on *I*) = 0.067). A total of 4955 reflections were assumed as observed applying the condition $I \geq 2\sigma(I)$. For **7′**, 10442 reflections were measured in the range 2.59° ≤ θ ≤ 32.38°, of which 5410 were non-equivalent by symmetry (R_{int}(on *I*) = 0.038). A total of 5324 reflections were assumed as observed applying the condition $I \geq 2\sigma(I)$. Lorentz-polarization but no absorption corrections were made.

The structures were solved by Direct methods, using SHELXS computer program (SHELXS-97)[34] and refined by full matrix least-squares method with SHELXL-97[35] computer program using 24866 reflections for **1**, 14224 reflections for **2**, 23062 reflections for **4**, 23600 reflections for **6**, and 10442 reflections for **7′** (very negative intensities were not assumed). The function minimized was $\sum||F_o|^2 - |F_c|^2|^2$, where for **1**, $w = [\sigma^2(I) + 0.0406P^2]^{-1}$, for **2**, $w = [\sigma^2(I) + (0.0827P)^2 + 0.2235P]^{-1}$, for **4**, $w = [\sigma^2(I) + (0.0252P)^2]^{-1}$, for **6**, $w = [\sigma^2(I) + (0.0746P^2)]^{-1}$, and for **7′**, $w = [\sigma^2(I) + (0.0515P)^2 + 0.4235P]^{-1}$, and $P = (|F_o|^2 + 2|F_c|^2)/3$ for all the structures. For **1**, **2**, and **6** all H atoms were computed and refined, using a riding model, with an isotropic temperature factor equal to 1.2 times of the atom which are linked. For **4** and **7′**, 10 H (**4**) or 4 H (**7′**) atoms were located from a difference synthesis and refined with an isotropic temperature factor equal to 1.2(**4**) or 1.5 (**5**) times of the atom which are linked. For both structures, 26 H atoms were computed and refined, using a riding model, with an overall isotropic temperature factor equal to 1.2 times of the atom which are linked.

The final $R(F)$ factor and $R_w(F^2)$ values as well as the number of parameters refined and other details concerning the refinement of the crystal structures are gathered in Table 3 and Table 4. CCDC 725389 (**1**), CCDC 725390 (**2**), CCDC 725391 (**4**), CCDC 725392 (**6**), and CCDC 725393 (**7′**) contain the supplementary crystallographic data for this paper. These data can be obtained free of charge from The Cambridge Crystallographic Data Centre via www.ccdc.cam.ac.uk/datarequest/cif.

Acknowledgment. This work has been financially supported by the Spanish Ministry of Culture and Education (Projects CTQ2007-63913) and by Generalitat de Catalunya (a grant to M.G.).

Supporting Information Available: ^{1}H NMR spectrum (250 MHz, 298 K, TMS) in CDCl$_3$ of complex **1** (Zn^{II}), complex **2**(Cd^{II}), and **L** ligand. This material is available free of charge via the Internet at http://pubs.acs.org.

(34) Sheldrick, G. M. *SHELXS-97, Program for Crystal Structure Determination*; University of Göttingen: Göttingen, Germany, 1997.

(35) Sheldrick, G. M. *SHELXL-97, Program for Crystal Structure Refinement*; University of Göttingen: Göttingen, Germany, 1997.